

Aus dem Institut für Klinische Diabetologie
Deutsches Diabetes-Zentrum
der Heinrich-Heine-Universität Düsseldorf

Direktor: Univ.-Prof. Dr. med. Michael Roden

**The role of diacylglycerol concentrations in the development of lipid-
mediated insulin resistance in human skeletal muscle**

Dissertation

zur Erlangung des Grades eines Doktors der Zahnmedizin
der Medizinischen Fakultät der Heinrich-Heine-Universität Düsseldorf

vorgelegt von

Janette Müller (geb. Decker)

2014

Als Inauguraldissertation gedruckt mit der Genehmigung der
Medizinischen Fakultät der Heinrich-Heine-Universität Düsseldorf

gez.: Univ.-Prof. Dr. med. Joachim Windolf
Dekan

Referent: Prof. Dr. Michael Roden

Korreferent: Prof. Dr. Dr. Thomas Beikler

Für meine Eltern

Teile dieser Arbeit wurden veröffentlicht:

Julia Szendroedi, Toru Yoshimura, Esther Phielix, Chrysi Koliaki, Melissa Marcucci, Dongyan Zhang, Tomas Jelenik, Janette Müller, Christian Herder, Peter Nowotny, Gerald I. Shulman, Michael Roden. C18-diacylglycerol species relate to muscle insulin resistance in humans. *Z. Zt. in Revision*

Zusammenfassung

Insulinresistenz ist ein häufiges Merkmal von Adipositas und Typ 2 Diabetes. Zahlreiche Mechanismen, wie Inflammation, Störungen der endothelialen und mitochondrialen Funktionen sowie im besonderen des Fettstoffwechsels, wurden bisher zur Erklärung der muskulären Insulinresistenz herangezogen. Getestet wurden die Hypothesen, dass (i) vermehrte Fettverfügbarkeit die Insulinsensitivität geschlechtsabhängig unterschiedlich hemmt und (ii) zur Zunahme von muskulären Lipidabbauprodukten führt, welche in der Folge neue PKC-Isoformen aktivieren und so Insulinresistenz verursachen.

Myocelluläre Lipidintermediate [Diacylglycerole (DAG), Ceramide] und Isoformen (β , δ , θ , ϵ) der Proteinkinase C (PKC) wurden während der parenteralen Verabreichung von Triacylglycerol (TAG) bzw. Glycerol bei gesunden Probanden untersucht. Der durch TAG-Infusionen bedingte Anstieg freier Fettsäuren (FFA) reduzierte den insulinstimulierten Gesamtkörper-Glukoseumsatz und die endogene (hepatische) Glukoseproduktion ohne Unterschiede zwischen männlichen und weiblichen Probanden. Die FFA-induzierte Insulinresistenz war mit einer frühzeitigen Zunahme der DAG Konzentration und einer nachfolgenden Aktivierung von PKC θ assoziiert. Im Gegensatz dazu blieb die Konzentration der Ceramide unverändert.

Die lipid-induzierte Insulinresistenz dürfte daher durch bestimmte DAG-Spezies vermittelt werden, die neue PKC-Isoformen aktivieren. Diese könnten die Insulinsignalübertragung hemmen und so die Glukoseintoleranz bei Adipositas und Typ 2 Diabetes begünstigen.

Summary

Insulin resistance is frequently correlated with obesity and type 2 diabetes. Up till now multiple mechanisms such as inflammation, endothelial and mitochondrial dysfunction and particularly lipid metabolism dysfunctions have been involved to elucidate muscle insulin resistance. Examined were the hypotheses that (i) increased lipid availability inhibits the insulin sensitivity gender-related and (ii) leads to an increase of muscle lipid-intermediates, which cause an activation of new PKC-isoforms and result in an insulin resistance.

Myocellular lipid-intermediates [diacylglycerol (DAG), ceramides] and protein kinase C (PKC) isoforms β , δ , θ , ϵ were examined during a triacylglycerol (TAG) or a glycerol infusion in healthy humans. Elevation of free fatty acids (FFA) caused by TAG infusions reduced the whole-body insulin-stimulated glucose disposal and endogenous (hepatic) glucose production without any difference between male and female volunteers. The FFA-induced insulin resistance was associated with an early increase of the DAG concentration and subsequently to an activation of the PKC θ . On the contrary, the ceramide concentration remained unchanged.

Lipid-induced insulin resistance may be initiated by the increase of DAG species resulting in the activation of new PKC-isoforms. This could inhibit the insulin signalling pathway and aggravate the glucose intolerance in obesity and type 2 diabetes.

Abbreviations

A	Arachidonate
ADP	Adenosine diphosphate
AKT	Protein B kinase
AS	Arachidonate/stearate
ATGL	Adipose triglyceride lipase
ATP	Adenosine triphosphate
BMI	Body mass index
BSA	Body surface area
CaCl₂	Calcium chloride
CD36	CD36, fatty acid translocase
CoA	Coenzyme A
CON	Control group
CPT 1	Carnitine palmitoyltransferase 1
CV	Intraassay or interassay variabilities
DAG	Diacylglycerol
DDZ	Deutsches Diabetes Zentrum
DANN	Deoxyribonucleic acid
EDTA	Ethylenediaminetetraacetic acid
EGP	Endogenous glucose production
EGTA	Ethylene glycerol tetraacetic acid
EKF	EKF Biosen C-Line
FA	Fatty acid
FAT	Fatty acid transport
FCCP	Carbonyl cyanide- <i>p</i> -trifluoromethoxyphenylhydrazone
FFA	Free fatty acids
G-6-P	Glucose-6-phosphate
HbA1c	Glycosylated haemoglobin
HCL	Hepatocellular lipids
HCL	Hydrochloric acid
HCS	Human chorionic somatomammotropin
HEPES	4-(2-hydroxyethyl)-1-piperazineethanesulfonic acid
HRR	High resolution respirometry

HSL	Hormone sensitive lipase
i.v.	Intravenous
IFG	Impaired fasting glycaemia
IGT	Impaired glucose tolerance
IL-6	Interleukin-6
IMCL	Intramyocellular lipids
IR	Insulin resistance
IRS-1	Insulin receptor substrate-1
L	Linoleate
LCA-CoA	Long chain acyl-coenzyme A
LIP	Lipid infusion group
MES	2-(N-morpholino)ethanesulfonic acid
MgCl₂	Magnesium chloride
MiR05	Mitochondrial respiration medium 05
Na₃VO₄	Sodium vanadate
NaCl	Sodium chloride
NaF	Sodium fluoride
NF-κB	Nuclear factor-kappaB
O	Oleate
OB	Obese
OGTT	Oral glucose tolerance test
OL	Oleate/linoleate
P	Probability value
P	Palmitate
PA	Palmitate/Arachidonate
PGC-1α	Peroxisome proliferator-activated receptor gamma coactivator-1α
PKC	Protein kinase C
PL	Palmitate/linoleate
PMSF	Phenylmethanesulfonylfluoride
PO	Palmitate/oleate
Pox	Protein oxidation rate
PPAR	Peroxisome proliferator-activated receptor
R_a	Rates of glucose appearance

R_d	Rates of glucose disappearance
REE	Resting energy expenditure
ROS	Reactive oxygen species
RQ	Respiratory quotient
S	Stearate
SD	Standard deviation
SEM	Standard error of the mean
Ser	Serine
SP	Stearate/palmitate
T1DM	Type 1 diabetes mellitus
T2DM	Type 2 diabetes mellitus
TAG	Triacylglyceride
TCA cycle	Tricarboxylic acid cycle; Krebs cycle
TNF-α	Tumor necrosis factor- α
USD	US-Dollar
VCO₂	Volume of carbon dioxide produced
VLDL	Very low density lipoprotein
VO₂	Volume of oxygen consumed
WHO	World Health Organisation

Table of Contents

List of Figures.....	VIII
List of Tables.....	VIII
1. Introduction.....	1
1.1 Obesity and overweight.....	1
1.1.1 Classification of obesity and overweight.....	1
1.1.2 Morbidity and mortality.....	2
1.2 Diabetes mellitus.....	3
1.3 Physiological effects of insulin.....	5
1.4 Cellular mechanisms of insulin resistance.....	7
2. Hypotheses.....	12
3. Methods.....	13
3.1 Volunteers and recruitment.....	13
3.2 Study protocols.....	13
3.2.1 FFA-IR group.....	13
3.2.2 Insulin signalling group.....	15
3.3 Hyperinsulinemic-euglycemic clamp.....	16
3.4 Oral glucose tolerance test.....	17
3.5 Measurement of the EGP.....	17
3.6 Indirect calorimetry.....	18
3.7 Skeletal muscle biopsy.....	18
3.8 Metabolites.....	19
3.9 High resolution respirometry.....	19
3.10 Myocellular lipid metabolites.....	20
3.11 Muscle protein kinase C activation.....	20
3.12 Calculations and statistics.....	21
4. Results.....	22
4.1 FFA-IR group.....	22
4.1.1 Plasma metabolites.....	22
4.1.2 Whole-body glucose metabolism.....	25
4.1.3 Myocellular lipid intermediates.....	29
4.1.4 Myocellular protein kinase C.....	32
4.2 Insulin signalling group.....	32
4.2.1 Plasma metabolites.....	32
4.2.2 Endogenous glucose production.....	36
4.2.3 Analysis of gender effects on EGP.....	36
5. Discussion.....	38

5.1	Effect of gender on whole-body glucose disposal and EGP	38
5.2	Effect of FFA on intracellular lipid intermediates	39
6.	Conclusion	43
	References.....	44

List of Figures

Figure 1. Physiology of the insulin effect.....	6
Figure 2. Cellular mechanism of lipid-induced insulin resistance.....	8
Figure 3. FFA-IR group.....	14
Figure 4. Insulin signalling group.....	16
Figure 5. Plasma free fatty acids (FFA-IR group).....	22
Figure 6. Plasma triglycerides (FFA-IR group).....	23
Figure 7. Plasma glycerol (FFA-IR group).....	24
Figure 8. Plasma insulin (FFA-IR group).....	24
Figure 9. Plasma C-peptides (FFA-IR group).....	25
Figure 10. Whole-body glucose disposal (unpaired).....	26
Figure 11. Analysis of gender effect (unpaired).....	27
Figure 12. Analysis of gender effect on BSA-value (unpaired).....	27
Figure 13. Analysis of gender effect (paired).....	28
Figure 14. Analysis of gender effect on BSA-value (paired).....	28
Figure 15. DAG cytosolic and membrane (paired).....	29
Figure 16. Cytosolic DAG species.....	30
Figure 17. Membrane DAG species.....	31
Figure 18. Myocellular ceramides (paired).....	31
Figure 19. PKC (paired).....	32
Figure 20. Plasma free fatty acids (insulin signalling group).....	33
Figure 21. Plasma triglycerides (insulin signalling group).....	33
Figure 22. Plasma glycerol (insulin signalling group).....	34
Figure 23. Plasma insulin (insulin signalling group).....	35
Figure 24. Plasma C-peptides (insulin signalling group).....	35
Figure 25. Endogenous glucose production.....	36
Figure 26. Endogenous glucose production gender-related.....	37

List of Tables

Table 1. Classification of overweight and obesity using BMI adapted from the WHO... 2	
Table 2. Volunteers' data of FFA-IR group.....	15
Table 3. Volunteers' data of insulin signalling group.....	16

1. Introduction

The increasing prevalence of obesity has reached epidemic proportions [1] with approximately 2-3 billion adults predicted to be overweight or obese in the year 2015 [2]. Obesity and physical inactivity, which result in a dysfunctional adipose tissue, can lead to lipid oversupply and increased flux of free fatty acids (FFA) into the skeletal muscle and an accumulation of intramyocellular triacylglycerides (TAG) [3]. Lipid oversupply raises concentrations of long chain acyl coenzyme A (CoA), diacylglycerol (DAG) and ceramides and can evolve a state of lipotoxicity causing cell dysfunction [4, 5]. Lipids can cause abnormal mitochondrial function consequently leading to oxidative stress [6] and to lower or incomplete fat oxidation [6-8] with subsequent TAG storage. Several studies have tried to elucidate the possible role of intramyocellular lipid accumulation in the development of insulin resistance. Both animal and human studies have provided evidence that TAG and FFA are associated with skeletal muscle insulin resistance. The mechanism linking obesity to the development of insulin resistance is not fully understood but it is known that insulin resistance is the best predictor for the development of type 2 diabetes (T2DM) [9] and it has become increasingly apparent that defects in skeletal muscle FA metabolism are involved [10].

1.1 Obesity and overweight

1.1.1 Classification of obesity and overweight

Obesity is a more extreme form of overweight and both are defined as abnormal or excessive fat accumulation that present a risk to health [11].

According to the World Health Organization (WHO) worldwide obesity has doubled since 1980 and 65% of the world's population live in countries where overweight and obesity kill more people than underweight [11]. Obesity can affect people of all ages and social groups. To identify and classify overweight and obesity a body mass index was introduced by Adolphe Quetelet in 1832 [12] and this has been used by the WHO since the early 1980s.

Body Mass Index (BMI) = body weight (kg)/[body height (m)]²

A BMI greater than 25 but less than 30 kg/m² is overweight.

A BMI of 30 kg/m² or greater is obesity.

BMI provides the simplest measure of overweight and obesity as it is the same for both sexes and for adult age groups across the entire world population. The WHO allocated a specific weight class to the BMI. The classification adapted from the WHO [13, 14] is shown in the **Table 1**.

Classification	BMI
Underweight	< 18.50 kg/m ²
Normal range	18.50 - 24.99 kg/m ²
Overweight	≥ 25.00 kg/m ²
Pre-obese	25.00 - 29.99 kg/m ²
Obese	≥ 30.00 kg/m ²
Obese class I	30.00 - 34.99 kg/m ²
Obese class II	35.00 - 39.99 kg/m ²
Obese class III	≥ 40 kg/m ²

Table 1. Classification of overweight and obesity using BMI adapted from the WHO Left column range from underweight to obese class III; right column the BMI range measured by the formula: body weight (kg)/[body height (m)]².

1.1.2 Morbidity and mortality

A fifth of all global deaths may result from overweight and obesity. This indicates that the mortality rate has increased 6 - 12 times in comparison to normal weight humans [11, 15]. But amazingly it has been proved that obesity may have some protective benefits. Paradoxically obese patients with cardiovascular diseases survive longer than their normal weight counterparts with cardiovascular diseases. Furthermore individuals who have normal weight at the diagnosis of diabetes have higher mortality rates than obese and overweight persons [16, 17]. Additionally the risk of cardiovascular mortality may be lower among individuals with high BMI and good aerobic fitness than individuals with normal BMI and poor fitness [16]. Carnethon et al. revealed that humans of lower body weight with obesity-related metabolic disorders may have underlying illnesses that predispose to mortality [17] and weight loss may be related to higher mortality [16]. On the contrary the cost of the comorbidities related to obesity in the USA are estimated to be 147 billion USD in 2008 [18] and 190 billion USD in 2012 [19] although the prevalence of obesity shows little change over the past 12 years. The data are consistent with the possibility of slight increases in 2009-2010 when the prevalence of obesity was 35.5% among adult men and 35.8% among adult women, with no significant change compared with 2003-2008; also in children and adolescents [20, 21]. In conclusion the risk of morbidity and mortality of diabetes is not generally dictated by lean, obese or

overweight conditions. It is to determine, if diabetes is a comorbidity of overweight and obesity and causes sequelae or is an underlying disease of lean weight conditions.

Overweight and obesity are often combined with insulin resistance, T2DM, cardiovascular diseases, joint diseases (osteoarthritis) and cancer (endometrial, breast and colon) [11]. The prevalence of diabetes in the United States and worldwide is increasing; e.g. 26 million US-American adults have diabetes, 79 million Americans aged 20 years or older have pre-diabetes and it is prophesied that 2050 nearly 50 million Americans will have diabetes [16].

The health risks associated with obesity combined with other diseases is classified dependent upon its origin [22]. The WHO published 2000 a risk evaluation. The risk is increased more than three times by diabetes mellitus, cholecytolithiasis, dyslipidaemia, insulin resistance and obstructive apnoea. The risk is increased two to three times by coronary, hypertension, arthrosis and gout and by a risk increase of one to two times carcinoma, polycystic ovary syndrome, infertility, dorsalgia and prenatal disorders are referred. The association between obesity and diabetes is well established because 90% of patients with T2DM show excess body weight [23].

1.2 Diabetes mellitus

The WHO defines diabetes mellitus as a chronic disease that occurs either when the pancreas does not produce enough insulin or when the body cannot effectively use the insulin it produces [15]. Insulin is a hormone of the β -cells of the Langerhans cells in the pancreas. Insulin is responsible for metabolic processes maintaining glucose homeostasis in the fed and the fasted state. Increased plasma glucose, FFA, branched-chain amino acids and incretins stimulate insulin release. Insulin has an anabolic effect on glucose, FA and amino acid storage as glycogen, TAG and protein [24]. In skeletal muscle and fat tissue, insulin stimulates glucose uptake causing a rapid decrease of blood glucose. In the liver, insulin suppresses gluconeogenesis, which leads to reduced endogenous glucose production (EGP) while stimulating glycogen synthesis. In the fasted state, insulin secretion is suppressed, so that lipolysis and glycogenolysis increase in order to ensure constant blood glucose levels. Diabetes mellitus is diagnosed in patients with increased plasma blood glucose at fasting (≥ 126 mg/dl) or a random plasma glucose ≥ 200 mg/dl (11.1 mmol/l) or glucose 2 h after ingestion of 75 g glucose (> 200

mg/dl) [25]. Impaired glucose tolerance (IGT) and impaired fasting glycaemia (IFG) (100 mg/dl – 125 mg/dl) often occur before the onset of overt T2DM [11, 25]. Diabetes mellitus is also diagnosed, when the glycosylated haemoglobin (HbA1c) level is \geq 6.5%. HbA1c provides a reliable measure of chronic glycaemia and correlates well with the risk of long-term diabetes complications [26]. Diabetes is classified into the following types:

- **Type 1 diabetes**

Type 1 diabetes mellitus (T1DM), previously known as insulin-dependent, juvenile or childhood-onset, is characterized by deficient insulin production and requires lifelong daily administration of insulin. Autoimmune processes are the cause of T1DM. Symptoms of the onset of T1DM include excessive excretion of urine (polyuria), thirst (polydipsia), constant hunger, weight loss, deterioration of vision and fatigue. Generally these symptoms occur suddenly [15].

- **Type 2 diabetes**

T2DM, formerly called non-insulin-dependent or adult-onset, results from the body's ineffective use of insulin and progressive β -cell failure. T2DM comprises of up to 90% of people with diabetes around the world, and is largely the result of excess body weight and physical inactivity combined with genetic predisposition. Symptoms may be similar to those of T1DM but are often less marked. As a result, the disease may not be diagnosed until several years after onset, when complications may already be present [15].

People with overt T2DM or increased risks of T2DM are mostly insulin resistant in skeletal muscle, liver and fat tissue [3]. Increased availability of FFA from diet and increased lipolysis rates of adipose tissue impair insulin signalling in skeletal muscle and the liver. Insulin resistance causes impaired glucose and utilization storage of glycogen in skeletal muscle and the liver. Additionally it increases release of glucose from the liver and increases lipolysis in the adipose tissue [27, 28]. Consequently, plasma glucose and FFA concentrations are frequently slightly increased in insulin resistant states.

- **Gestational diabetes**

Gestational diabetes is defined as any form of hyperglycaemia with onset or first recognition during pregnancy. Women have an increased risk of gestational diabetes, if they

are e.g. overweight, have a family predisposition for diabetes and their own birth weight was > 4000 g [29]. Pregnancy is a condition characterized by progressive insulin resistance, starting in the second part of pregnancy and progressing through the third trimester [30]. During the second part of pregnancy specific hormones are produced to increase the demand of energy in form of glucose. The placenta produces human chorionic somatomammotropin (HCS) and free cortisol, oestrogen and progesterone. HCS stimulates insulin secretion in the foetus and inhibits peripheral maternal glucose uptake. In the progress of pregnancy both the size of the placenta and secretion of hormones increase and leads to a higher insulin resistant state [30]. If the pancreas is unable to compensate the increased glucose concentration, an absolute insulin resistance develops. The majority of women are able to raise their own insulin production during latter part of pregnancy without being sensitive to insulin, thus a relative insulin resistance exists. Women with gestational diabetes have increased risk for T2DM [15].

1.3 Physiological effects of insulin

During the fed and the fasted state metabolic processes maintaining glucose homeostasis are determined by insulin. Under postprandial conditions, insulin acts as an anabolic hormone by favouring glucose lipid and protein storage. The glucose homeostasis regulates these metabolic processes throughout the fed and fasted states [24].

Insulin regulates glucose uptake and circulating FFA concentrations. In adipose tissue insulin decreases lipolysis and reduces FFA efflux from adipocytes; in liver insulin inhibits gluconeogenesis by reducing key enzyme activities and in skeletal muscle induces glucose uptake by stimulating the translocation of GLUT 4 glucose transporter to the plasma membrane [31].

Insulin effect during the fed and fasted state

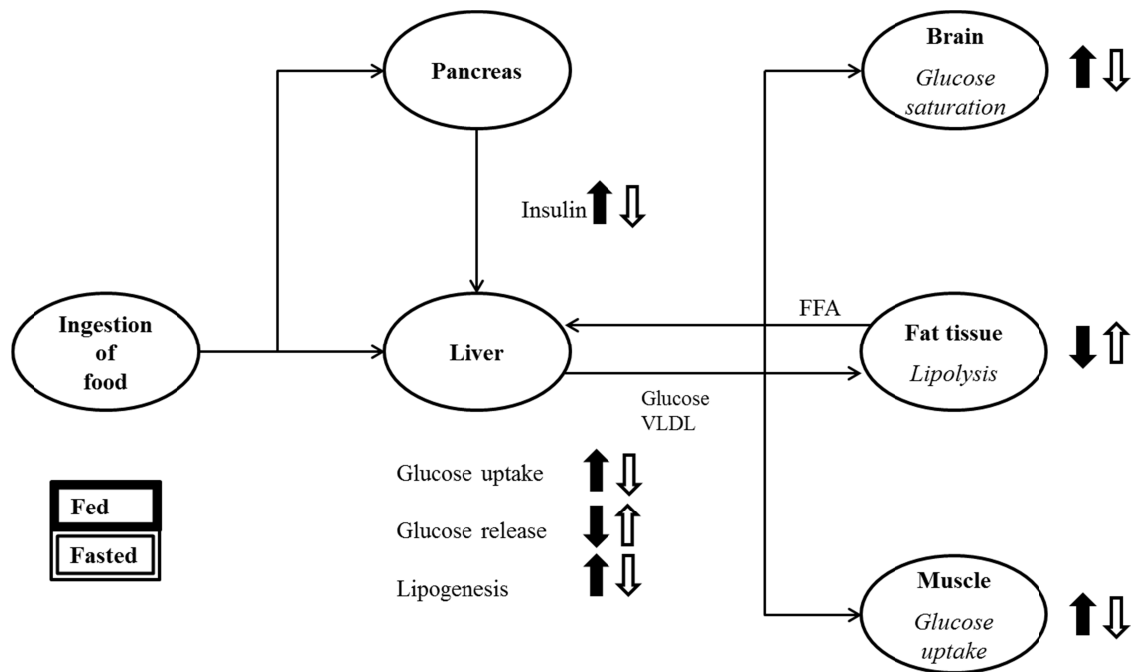


Figure 1. Physiology of the insulin effect Metabolic changes in the fed and in the fasted state. Black arrows describe the effect of insulin during fed and white arrows during the fasted state [Adapted from Szendroedi, J., et al., Nature Rev Endocrinol. 2011 [3]].

Figure 1 depicts the main pathways of energy metabolism regulated by insulin in the fasted and fed state. Nutrients are absorbed in the intestine and lead to insulin secretion. Insulin stimulates glucose uptake in insulin responsive tissues, glycogen synthesis in the liver and skeletal muscle, and lipogenesis in the adipose tissue and additionally initiates satiety signals in the brain and inhibits glucose output of the liver and of lipolysis in fat tissue. Substrates are oxidized in the mitochondria to supply energy demand.

Whole-body insulin sensitivity can be measured from whole-body glucose uptake by the gold standard method, the hyperinsulinemic euglycemic clamp [32]. Tissue specific insulin sensitivity is assessed from glucose clearance by skeletal muscle, in the liver from insulin-mediated suppression of EGP and in adipose tissue from suppression of lipolysis by hyperinsulinemia.

1.4 Cellular mechanisms of insulin resistance

Insulin resistance is defined as impaired whole-body glucose disposal during insulin stimulation when the majority of glucose is disposed in skeletal muscle and almost exclusively metabolized non-oxidatively to glycogen [33]. Alternatively it is simplified as an impaired sensitivity to insulin of its main target (e.g. adipose tissue, liver and skeletal muscle) [31]. The cellular mechanism may be a defect of the insulin receptors, rarely congenital syndromes (e.g. Johanson-Blizzard syndrome [34] or Alstrom syndrome [35]), or a defect of the metabolism of the insulin receptor. Especially mutations in the insulin receptor gene cause severe insulin resistant syndromes, e.g. leprechaunism, Rabson-Mendenhall syndrome [36] and type A insulin resistance syndrome [37]. Rabson-Mendenhall syndrome is defined as autosomal recessive conditions in which both alleles for the insulin receptor are abnormal, and patients fail to respond to endogenous and exogenous insulin [36].

Lettner and Roden revealed that the development of cellular insulin resistance may be associated with accelerated release of fat from adipocyte and intracellular accumulation of toxic lipid metabolites (e.g. lipotoxicity), secondly with an imbalanced release of adipocytokines from adipocytes (e.g. adiponectin/ TNF- α ratio) and thirdly chronic low-grade inflammation and release of cytokines [38]. The cellular mechanisms of glucose-, inflammation- or lipid-induced insulin resistance are depicted in **Figure 2**.

Thus, insulin resistance occurs in association with gene defects (e.g. syndromes), a variety of physiological (e.g. pregnancy) and pathophysiological states.

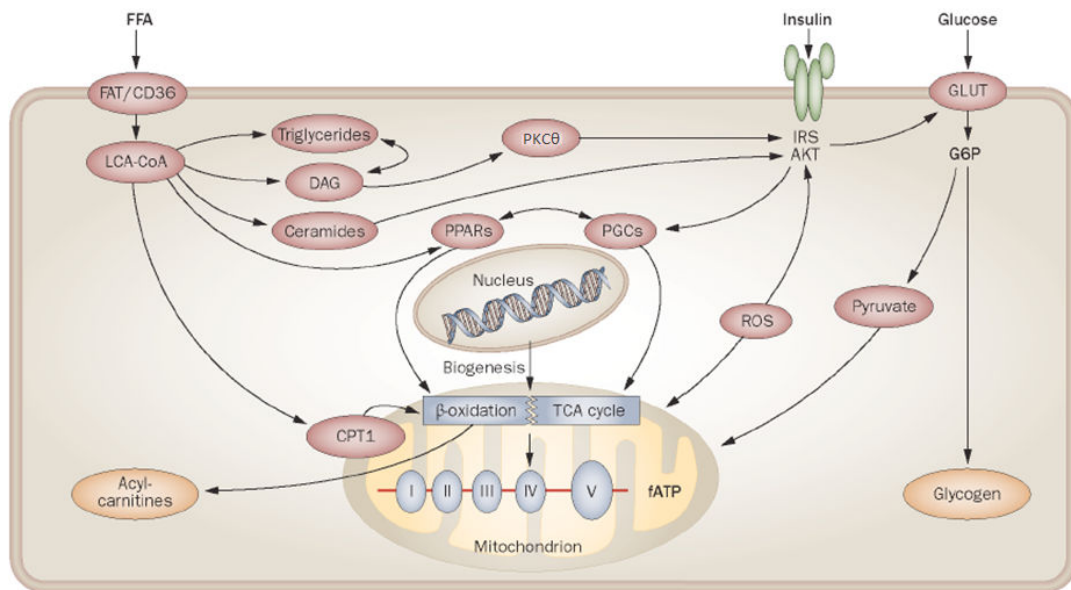


Figure 2. Cellular mechanism of lipid-induced insulin resistance

FFA: free fatty acids; FAT/CD 36: fatty acid transport protein/CD 36 fatty acid translocase CD36; LCA-CoA: Long chain acyl-coenzyme A; DAG: Diacylglycerol; PKC θ : Protein kinase c θ ; PPARs: peroxisome proliferator-activated receptors; PGCs: Peroxisome proliferator-activated receptor gamma coactivator 1-alpha; IRS: insulin receptor; AKT: Protein kinase B; GLUT: Glucose transporter; G6P: Glucose-6-Phosphat; ROS: reactive oxygen species; CPT1: Carnitine palmitoyltransferase I; TCA cycle: tricarboxylic acid cycle. FFA enter via FAT and CD36 and increase the LCA-CoA.

[Modified from Szendroedi, J., et al., Nat Rev Endocrinol. 2011 [3]]

Glucose-induced insulin resistance is known as glucose toxicity [39]. This has been revealed in rodents, which were infused with glucose and showed an impaired insulin action in skeletal muscle [39-43]. Hoy revealed that 5 h of glucose infusion induces skeletal muscle insulin resistance [39]. Further, this was associated with an increase in DAG and malonyl-CoA levels in skeletal muscle [39]. Insulin-stimulated glucose transport occurs via a PI3-kinase-Akt-dependant pathway; resulting in translocation of the GLUT4 to the plasma membrane to facilitate glucose uptake [39]. Houdali et al. supported the hypothesis that continuous glucose infusion induced translocation of GLUT4, while the early steps of the insulin signalling cascade were not increased. He proposed that these effects could be mediated by activation of PKC. Continuous glucose infusion induced GLUT4 protein release and translocation to the plasma membrane [41].

In recent years it has become increasingly apparent that obesity and insulin resistance are associated with a state of chronic low-grade inflammation [31, 44-46]. Obese patients with a chronic low-grade inflammation have increased plasma levels of C-reactive protein, inflammatory cytokines such as TNF- α . Inflammatory-induced insulin re-

sistance was first revealed by Hotamisligil et al. and Karasik et al [47]. It was shown that proinflammatory cytokine TNF- α was able to induce insulin resistance. Increased levels of markers and mediators of inflammation and acute-phase reactants such as fibrinogen, C-reactive protein (CRP), IL-6, plasminogen activator inhibitor-1 (PAI-1), sialic acid, and white cell count may correlate with T2DM [47]. Zeyda and Stulnig described that neutralizing TNF- α in rats provided first compelling evidence that inflammatory mediators could cause insulin resistance [31, 48] and also in vitro experiments with cultured murine adipocytes demonstrated TNF- α was linked to insulin resistance [31]. Another consideration is that increased systemic levels of cytokines, e.g. IL-6 and TNF- α , impaired myocellular mitochondrial function and/or increased reactive oxygen species (ROS) production (oxidative stress), may lead to lipid accumulation and subsequently to insulin resistance.

This resulted in incomplete β -oxidation, increase of acyl-carnitines and oxidative stress raising reactive oxygen species along with activation of atypical PKC isoforms and the pro-inflammatory NF- κ B [8, 49, 50]. It has been determined that fatty acids are only converted to acetyl-CoA but not via the TCA cycle because of a lack of oxaloacetate during reduced intake of glucose and an increased lipolysis. Lipid overflow, subclinical inflammation (cytokines) and/or abnormal mitochondrial function may exacerbate insulin resistance.

It has been reported that patients suffering from overweight or obesity often show abnormalities in their mitochondrial structure such as paracrystalline inclusions, typical of mitochondriopathies [51, 52]. Skeletal muscle strongly relies on mitochondrial oxidative phosphorylation for ATP production. Accordingly decreased oxidative capacity and mitochondrial aberration may be major contributors to the development of insulin resistance and T2DM and can be discerned in skeletal muscle biopsies of insulin resistant humans [53]. Thus, an insulin resistance may lead to impaired mitochondrial fitness with disorders of the availability of energy in form of ATP, to a production of toxic ROS and to inflammatory cell reactions [52, 54].

Plasma FFA flux is related to whole-body lipolysis [55] and is frequently increased in obesity and T2DM. In the last few years the evidence has been accumulated that increased levels of FFA are associated with insulin resistance [56]. Further it is revealed that FFA may inhibit insulin signalling by increasing serine phosphorylation of insulin

receptor-1 (IRS-1). Elevation of plasma FFA in normal weight patients via lipid infusion reduces reversibly glucose transport and/or phosphorylation [49, 57]. According to the scheme depicted in **Figure 1** in the insulin resistant state, glucose uptake and glycogen synthesis are impaired and consequently plasma glucose levels are high. Parallel insulin levels are extremely high and promote lipid deposits in the adipose tissue but also in the non-adipose tissue, which is called ectopic lipid deposition. The accumulation of ectopic lipids (intramyocellular and hepatocellular lipids, IMCL, HCL) is often related to a lipid-induced insulin resistance [4, 9, 58, 59]. This is the result of increased availability of lipids, caused by less physical activity and a high caloric nutrition.

Randle et al. postulated that increased FFA oxidation inactivates pyruvate dehydrogenase with subsequent inhibition of phosphofructokinase [60]. This causes intracellular glucose-6-phosphate (G-6-P) to rise which can decrease hexokinase II activity with consequent decreased glucose uptake and glycogen synthesis [27]. To examine the mechanism in which lipids cause insulin resistance Roden et al. ascertained that on the contrary to the original postulated mechanism, - FFA inhibit insulin stimulated glucose uptake in muscle through initial inhibition of pyruvate dehydrogenase -, the FFA-induced insulin resistance is induced by initial inhibition of glucose transport/phosphorylation [57, 61].

Plasma FFA are transported via fatty acid transporters (FAT)/CD36 into the cell and the elevated lipid metabolites are converted to acyl-CoA, TAGs, ceramides and DAG or are hydrolysed. DAG are by-products of lipolysis consecutive to TAG hydrolysis by adipose triglyceride lipase (ATGL) and are subsequently hydrolysed by hormone-sensitive lipase (HSL) [4]. Previous studies suggested that insulin resistance is caused by raised intracellular lipid metabolites such as DAG and ceramides [8, 49, 50, 59]. The accumulated TAGs are metabolically inert but lipid metabolites such as DAG and ceramides inhibit insulin signalling [59, 62].

Animal studies revealed that lipid-induced insulin resistance is caused by intramyocellular DAG-induced stimulation of protein kinase C (PKC) which leads to activation of the atypical isoform PKC θ [63], resulting in a serine phosphorylation of IRS-1. Accumulation of DAG may be caused by an imbalance of ATGL relative to HSL. Consequently the imbalance of ATGL relative to HSL may increase intracellular DAG concentration and finally enhance insulin resistance. Other studies challenge the

DAG hypothesis with respect to the sequence of events promoting insulin resistance in suggesting that myocellular ceramides and ceramidase activity are the primary culprits instead of the DAG [64]. Ceramides might have a direct inhibiting influence on IRS-1 and AKT-phosphorylation. Accordingly the role of the DAG, activating isoforms of the PKCs, needs to be examined. In humans the pathway and the relative roles of ceramides and DAGs are still unclear and have to be explored.

2. Hypotheses

- Short-term elevation of plasma FFA increases myocellular DAG prior to activation of novel PKC isoforms and leads to an induction of insulin resistance. Insulin resistance is primarily caused by DAG and not by increased myocellular ceramides.
- DAG species, inducing an insulin resistance, are localized in the membrane and not in the cytosol.
- M-value and EGP are not affected by gender under conditions of lipid-induced insulin resistance.

Two cohorts were selected to confirm the hypotheses. The FFA-IR group (lipid-induced insulin resistance) had to reveal primarily the effect of lipids on fatty acid intermediates inducing an insulin resistance and secondly the sequence of events leading to a lipid-induced insulin resistance. The insulin signalling group had to reveal a lipid impaired insulin signalling but is not part of the dissertation.

3. Methods

3.1 Volunteers and recruitment

Normal weight and healthy participants were recruited by research group of the department for Clinical Diabetologie of the German Diabetes Centre (DDZ), Heinrich Heine University Düsseldorf.

All participants had to give a written consent, which was registered (ClinicalTrials.gov Identifier number: NCT01229059 approved by the local institutional ethics board) and performed according to the Declaration of Helsinki. 23 normal weight glucose tolerant and insulin sensitive volunteers without family history of diabetes were included. The data of the subjects are summarized in **Table 2 and Table 3**.

3.2 Study protocols

The participants underwent two experimental conditions in random order to examine lipid-induced insulin resistance. We divided the volunteers in two study groups, (i) FFA-IR group and (ii) the insulin signalling group. The 16 volunteers took part in the FFA-IR group and 7 in insulin signalling group. The participants were given in a random order lipid or glycerol infusion over 6 h and a hyperinsulinemic-euglycemic clamp was taken (**Figure 3 & Figure 4**). Muscle biopsies were taken before (FFA-IR group) and before and during (insulin signalling group) the hyperinsulinemic-euglycemic clamp to reveal the lipid-induced insulin resistance and insulin signalling pathway. The FFA-IR group was selected to determine the sequence of events leading to a lipid-induced insulin resistance and to examine the relevance of fatty acids intermediates to insulin resistance. The aim of the insulin signalling group was to reveal a lipid impaired insulin signalling, but is not part of this dissertation.

3.2.1 FFA-IR group

The participants were instructed to fast overnight for about 10 h. In the morning (7:00 a.m.) deuterated glucose was infused to determine basal EGP [65, 66]. In order to induce insulin resistance, a lipid-rich infusion (Intralipid[®]; Fresenius Kabi GmbH, Bad Homburg, Germany) was applied (-240 until -230 min: 10 ml/h; -229 until +150 min: 90 ml/h). On another occasion 2.5% glycerol dissolved in 0.9% saline (Fresenius Kabi

GmbH) was infused (-240 min until -230 min: 10 ml/h; -229 until +150 min: 90 ml/h) as a control experiment. At baseline, 2.5 and 4 h after the start of the lipid/glycerol infusion a muscle biopsy was taken to study lipid metabolites, translocation of PKC isoforms β , δ , θ , ε and mitochondrial functions. To standardize fasting conditions a pancreatic clamp was performed. After 6 h insulin sensitivity of skeletal muscle and the liver were measured by using hyperinsulinemic-euglycemic clamp test (0 until +150 min) in combination with the infusion of [$^2\text{H}_2$]glucose (-360 until +150 min). The substrate oxidation was assessed by indirect calorimetry at baseline and during the hyperinsulinemic clamp (**Figure 3**).

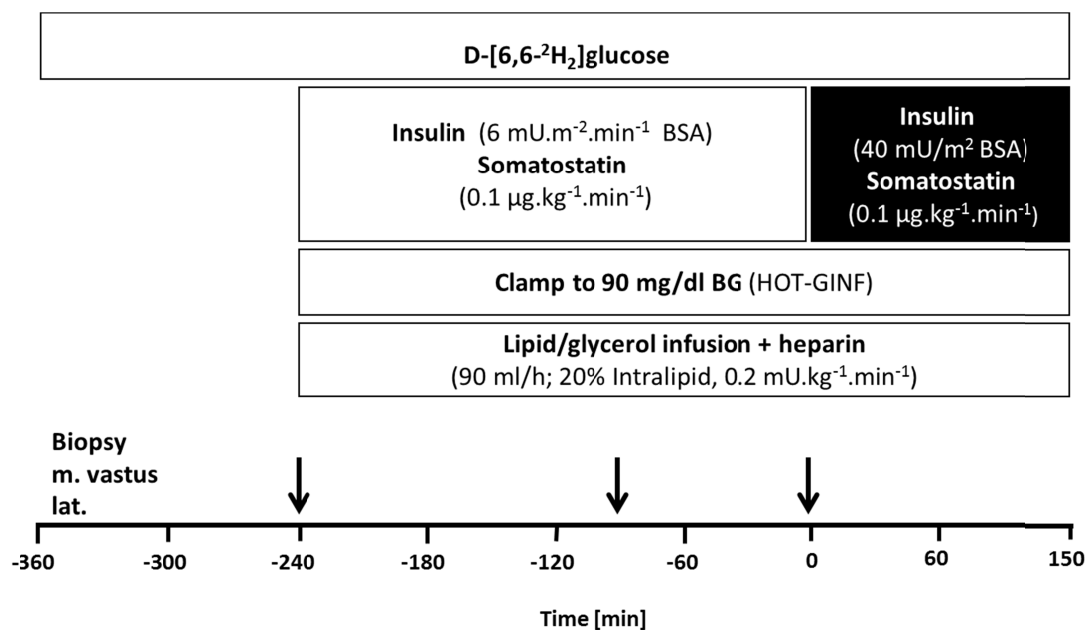


Figure 3. FFA-IR group 11 male and 5 female volunteers participated in this study. Muscle biopsies were taken at -240 min, -90 min and 0 min (black arrow).

The data of the sixteen young, lean, healthy, glucose-tolerant, untrained (sedentary) humans are summarized in **Table 2**.

n total (male/female)	16 (11/5)
Age (years)	28.88 ± 5.33
Body mass index (kg/m ²)	23.60 ± 2.03
Fasting glucose (mg/dl)	81.74 ± 24.25
Fasting FFA (mmol/l)	0.43 ± 0.19
Fasting triglycerides (mg/dl)	83.69 ± 30.70
HbA1c (%)	5.33 ± 0.28
Baecke Index	2.78 ± 0.47

Table 2. Volunteers' data of FFA-IR group 11 male and 5 female volunteers participated in this study group. Means were given ± SD.

Additionally to the plasma values, the Baecke Index is listed in **Table 3**. Baecke et al. developed 1982 a questionnaire for evaluating a person's physical activity and separating it into three distinct dimensions. The three dimensions were physical activity at work, sport during leisure time and other physical activity during leisure time [67]. The volunteers had to rate themselves and gave points to different questions based upon their activities. The sum of these points was mean valued.

3.2.2 Insulin signalling group

The participants were instructed to fast overnight for about 10 h. In the morning (7:00 a.m.) deuterated glucose was infused to determine basal endogenous glucose production [65, 66]. In order to induce insulin resistance a lipid rich infusion (Intralipid®; Fresenius Kabi GmbH, Bad Homburg, Germany) was applied (-240 until -230 min: 10ml/h; -229 until +150 min: 90 ml/h). On another occasion, as a control experiment 2.5% glycerol dissolved in 0.9% saline (Fresenius Kabi GmbH) was infused (-240 min until -230 min: 10ml/h; -229 until +150 min: 90 ml/h). To standardize fasting conditions a pancreatic clamp was performed, and after 6 h insulin sensitivity of skeletal muscle and liver were measured using the hyperinsulinemic-euglycemic clamp test (0 until +150 min) combined with the infusion of [²H₂]glucose (-360 until +150 min). To examine the insulin signalling, a muscle biopsy was taken from the lateral thigh (m. vastus lateralis) at baseline after 1.5 h lipid or glycerol infusion and 30 min after starting the hyperinsulinemic clamp. The substrate oxidation was assessed from indirect calorimetry at baseline and during the hyperinsulinemic clamp (**Figure 4**).

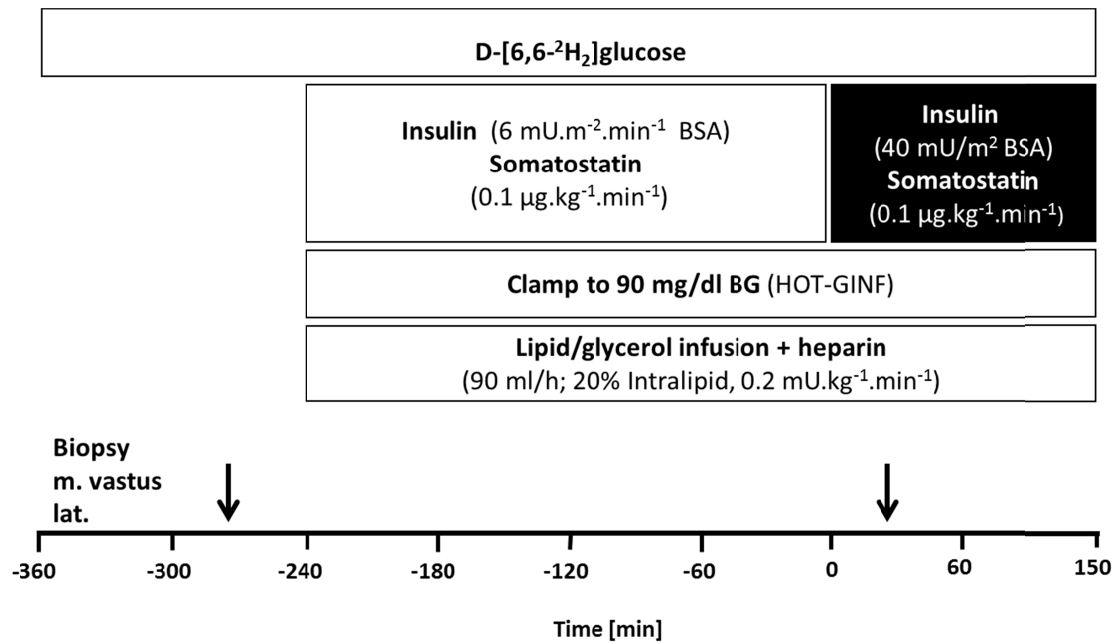


Figure 4. Insulin signalling group 4 male and 3 female volunteers participated in the study. Muscle biopsies were taken at -270 min and +30 min (black arrow).

The data of the seven young, lean, healthy, glucose-tolerant, untrained (sedentary) humans are summarized in **Table 3**.

n total (male/female)	7 (4/3)
Age (years)	23.75 ± 1.49
Body mass index (kg/m ²)	23.28 ± 1.88
Fasting glucose (mg/dl)	75.36 ± 9.03
Fasting FFA (mmol/l)	0.39 ± 0.39
Fasting triglycerides (mg/dl)	111.71 ± 69.90
HbA1c (%)	5.04 ± 0.19
Baecke Index	2.80 ± 0.33

Table 3. Volunteers' data of insulin signalling group 4 male and 3 female volunteers participated in the study. Means were given ± SD.

3.3 Hyperinsulinemic-euglycemic clamp

The hyperinsulinemic-euglycemic clamp was performed to standardize fasting insulin levels and assess the whole-body glucose uptake [68, 69]. After overnight fasting, studies began at 7:00 a.m. with insertion of catheters (Vasofix; Braun, Melsungen, Germany) in antecubital veins of both arms to allow for blood sampling and infusions. 5 min

before the clamp a continuous infusion of Somatostatin ($0.1 \mu\text{g}\cdot\text{kg}^{-1}\cdot\text{min}^{-1}$, UCB Pharma) was given in order to inhibit the endogen insulin and glucagon secretion.

In a two-step continuous insulin infusion (Actrapid, Novo Nordisc, Bagsvaerd, Denmark) insulin resistance was determined. The prime stage was at a low level (-240 until 0 min) $6 \text{ mU}/\text{m}^2 \text{ body surface min}^{-1}$ and the second at a high level (0 until +150 min): $40 \text{ mU}/\text{m}^2 \text{ body surface min}^{-1}$.

The glucose infusion was adjusted at 5 min intervals based on the actual plasma glucose concentration. To maintain stable enrichments of $[6.6\text{-}^2\text{H}_2]$ glucose during the clamp tests, the variable glucose infusion was enriched to 2% with $[6.6\text{-}^2\text{H}_2]$ glucose. In regular intervals during the clamp test blood withdrawals were taken to determine the amount of hormone, adipokines, cytokines and lipids. These techniques determine the quantity of glucose disposal and EGP.

3.4 Oral glucose tolerance test

Each fasted proband drank within 5 min 300 ml glucose solution. Then still in fasting conditions the insulin plasma concentration, C-peptide, inflammation markers and adipokines were tested after 10, 20 and 30 min and then for the next 180 min in a half hourly rhythm to evaluate the blood sugar rates [70]. Parallel blood tests were taken to characterize the gene expressions in whole blood (non-gene analysis and non DNA conservation).

3.5 Measurement of the EGP

To assess endogenous glucose production each fasted participant was given per i.v. $[^2\text{H}_2]$ glucose. The infusion began with a 99.9% enriched deuterated glucose. After 3 h an additional dose ($1.19 \text{ mg}/\text{kg}$ bodyweight) was given for 5 min with a further infusion. A gas chromatography and mass spectrometry were carried out to determine the quantity of $[^2\text{H}_2]$ glucose in plasma and the elimination of proteins.

3.6 Indirect calorimetry

The amount of sugar and fat burned was calculated of the whole-body energy and were checked by each participant before the test began and ended. A transparent cover was placed over the participant's head and the exhaled breath was analysed by adding fresh air. Indirect calorimetry was performed in the canopy mode using Vmax Encore 29 n [equipment for pulmonary function measuring spirometry (CareFusion, Höchberg, Germany)] at baseline, at the end of intervention and during steady-state clamp conditions over a period of 20 min after 10 min of adaptation to the setting. Rates of oxygen uptake (VO_2) and carbon dioxide disposal (VCO_2) were measured and respiratory quotient (RQ) [71] and REE were calculated using abbreviated Weir equation. Substrate oxidation was calculated according to Frayn [71] with fixed estimated protein oxidation rate (Pox) of 15% of REE: Carbohydrate oxidation rate (mg/kg min) = $[(4.55 \cdot \text{VCO}_2) - (3.21 \cdot \text{VO}_2) - 0.459 \cdot \text{Pox}] \cdot 1000 / \text{kg body weight}$; where VCO_2 is carbon dioxide production and VO_2 is oxygen consumption; and lipid oxidation rate (mg/kg min) = $[(1.67 \cdot \text{VO}_2) - (1.67 \cdot \text{VCO}_2) - 0.307 \cdot \text{Pox}] \cdot 1000 / \text{kg body weight}$. Non-oxidative glucose disposal was calculated from the difference between R_d and carbohydrate oxidation.

3.7 Skeletal muscle biopsy

When the patient lay in a supine and resting position, the selected muscle (m. vastus lateralis) region was subcutaneously anaesthetised with a local anaesthetic (Xylocain[®] 2%). After testing the anaesthetised region with a needle, a cut of about 5 mm was made with a scalpel. The subcutaneous fat tissue and muscle fibres were obtained using a modified Bergström biopsy needle with suction. The excision region for the subcutaneous fat tissue was the abdomen and the lateral thigh (m. vastus lateralis) for the muscle fibre. The cut was connected with steri-strips and bandaged. The patient had to check the wound for approximately two weeks. All samples were kept in liquid nitrogen until analysis had occurred. Biopsies were homogenized in six volumes of lysis buffer containing 50 mmol/l HEPES, pH 7.5, 137 mmol/l NaCl, 1 mmol/l CaCl_2 , 1 mmol/l MgCl_2 , 10% glycerol, 2 mmol/l EDTA, 10 mmol/l NaF, 2 mmol/l Na_3VO_4 , and protease inhibitor cocktail. Muscle homogenates were solubilized in 1% NP-40 for 1 h at 4 °C and centrifuged at 14.000 g for 10 min.

3.8 Metabolites

190 ml blood was taken to determine parameter of glucose, lipid metabolism, hemogram, (blood glucose, insulin, C-peptide, triglyceride, FFA, glycerol, glucagon) and serological immune mediators. Blood samples were immediately chilled, centrifuged and supernatants stored at -20 °C until analysis. Venous blood glucose concentration was measured immediately using the glucose oxidase method (EKF Biosen C-Line glucose analyzer, EKF diagnostic GmbH, Barleben, Germany) [72]. FFA were assayed with the microfluorimetric method (intraassay CV < 1%, interassay CV 2.4%; Wako, Neuss, Germany) after prevention of in vitro lipolysis by collecting blood into vials containing orlistat [53]. Serum TAG, cholesterol and liver transaminases were analyzed by enzymatic assays (Hitachi analyzer, Roche Diagnostics, Mannheim, Germany).

3.9 High resolution respirometry

Ex vivo mitochondrial function was assessed with high resolution respirometry (HRR) as described [73]. Fresh muscle samples were rapidly put in ice-cold BIOPS buffer (2.77 mmol/l CaKEGTA, 7.23 mmol/l KEGTA, 5.77 mmol/l NaATP, 6.56 mmol/l MgCl₂-6H₂O, 20 mmol/l taurine, 15 mmol/l Na-phosphocreatine, 20 mmol/l Imidazole, 0.5 mmol/l DTT, 50 mmol/l MES, pH 7.1). Muscle fibres (1-2 mg) were trimmed off connective tissue muscle and permeabilized with saponin (50 µg/ml) in ice-cold BIOPS buffer at 4 °C for 25 min. Then, the samples were washed twice in ice-cold MiR05 buffer [0.5 mmol/l EGTA, 3 mmol/l MgCl₂-6 H₂O, 60 mmol/l K-lactobionate, 20 mmol/l taurine, 10 mmol/l KH₂PO₄, 20 mmol/l HEPES, 110 mmol/l sucrose, 1 g/l fat-free BSA (body surface area), pH 7.1] for 10 min. HRR of permeabilized fibres was performed in MiR05 buffer at 37 °C and 200-400 µM oxygen to avoid limitation of oxygen supply (Oxygraph-2k, Oroboros Instruments, Innsbruck, Austria). Defined respiratory states were obtained by the following multiple substrate-inhibitor titration protocol: 2 mmol/l malate, 10 mmol/l pyruvate, 10 mmol/l glutamate and 2.5 mmol/l ADP for state 3 respiration of complex I, 10 mmol/l succinate for combined state 3 respiration of complex I and II, 10 µmol/l cytochrome c for mitochondrial membrane integrity check, carbonyl cyanide-*p*-trifluoromethoxyphenylhydrazone (FCCP) (stepwise increments of 0.25 µmol/l up to the final concentration of max. 1.25 µmol/l) for maximal respiratory capacity, namely state u, and 2.5 µmol/l antimycin A. Addition of cyto-

chrome c did not increase oxygen consumption indicating integrity of the outer mitochondrial membrane after saponin permeabilization.

3.10 Myocellular lipid metabolites

For DAG extraction, muscle tissue was homogenized in a buffer solution (20 mmol/l Tris-HCl, 1 mmol/l EDTA, 0.25 mmol/l EGTA, 250 mmol/l sucrose, 2 mmol/l PMSF) containing a protease inhibitor mixture (Roche), and samples were centrifuged at 100.000 g for 1 h. The supernatants containing the cytosolic fraction were collected. DAG levels were then measured as previously described [74]. Total cytosolic DAG content is expressed as the sum of individual species. Ceramides were measured as previously described [75].

3.11 Muscle protein kinase C activation

PKC is a family of structurally and functionally related proteins derived from multiple genes after alternative splicing [56]. In response to the increasing DAG or tumor promoting agents, PKC is activated. There are 12 isozymes of PKC characterized. These are classified into three groups: classical (cPKC α , β I, β II, γ), novel (nPKC δ , ϵ , θ , η) and atypical isoforms (aPKC ζ , ι/λ) [56]. PKC isoforms regulate diverse cellular signalling pathways by phosphorylating their downstream kinases and substrate proteins. The PKC can translocate during activation from the cytosol to the cell membrane. The amount of which isoform of PKC is found in the membrane is a measure of its activation.

Membrane translocation for the different PKC isoforms (PKC β , ϵ , δ , θ) was assessed as described previously [74]. Both membrane and cytosol proteins were detected on the same film with enhanced chemiluminescence in the same exposure time. PKC translocation was expressed as the ratio of arbitrary units of membrane bands over cytosol bands. Membrane band density was corrected by Na⁺/K⁺-ATPase band density and cytosolic band density was corrected by glyceraldehyde 3-phosphate dehydrogenase band density [74]. The advantage of band density is that it permits the location and identification of proteins in gels.

3.12 Calculations and statistics

Basal rates of glucose appearance (R_a) were calculated by dividing the tracer [6,6- $^2\text{H}_2$]glucose infusion rate times tracer enrichment by the per cent of tracer enrichment in plasma and subtracting the tracer infusion rate [76]. R_a was calculated using Steele's non-steady state equations [77]. EGP was calculated from the difference between R_a and mean glucose infusion rates. All statistical analyses were performed using SPSS 6.0 software (SPSS Inc., Chicago, IL, USA). Data are presented as means \pm SD or SEM throughout the text and in the figures. The SEM value was calculated for figures 5-26; the SD was taken for table II and III. Statistical comparisons between study groups were performed using ANOVA and repeated measurements ANOVA with Tukey post hoc testing when appropriate. Within-group differences were determined using two-tailed Student's *t* tests. Non-parametric correlations are Spearman correlations (*p*). Differences were considered significant at the 5% level.

4. Results

4.1 FFA-IR group

The plasma values of the volunteers were measured once during lipid infusion and secondly during glycerol infusion (**Figure 3**) to examine the lipid-induced insulin resistance. The glycerol infusion served as control (CON). Results are shown in following figures (**Figures 5 - 19**).

4.1.1 Plasma metabolites

Lean, healthy, young humans were given a triglyceride rich infusion [(LIP) n = 16] and at a later date glycerol infusion [(CON) n = 7] over 9 h. A hyperinsulinemic-euglycemic clamp started after 6 h (0 min). FFA concentration during the lipid infusion constantly increased after 90 min ($*p < 10^{-6}$) and after 5 h ($**p < 10^{-6}$). At a peak at -60 min and after starting clamp (0 min) the graph slightly decreased ($***p < 0.0003$). The FFA concentration during the glycerol infusion remained almost constant ($p < 0.0005$) (**Figure 5**).

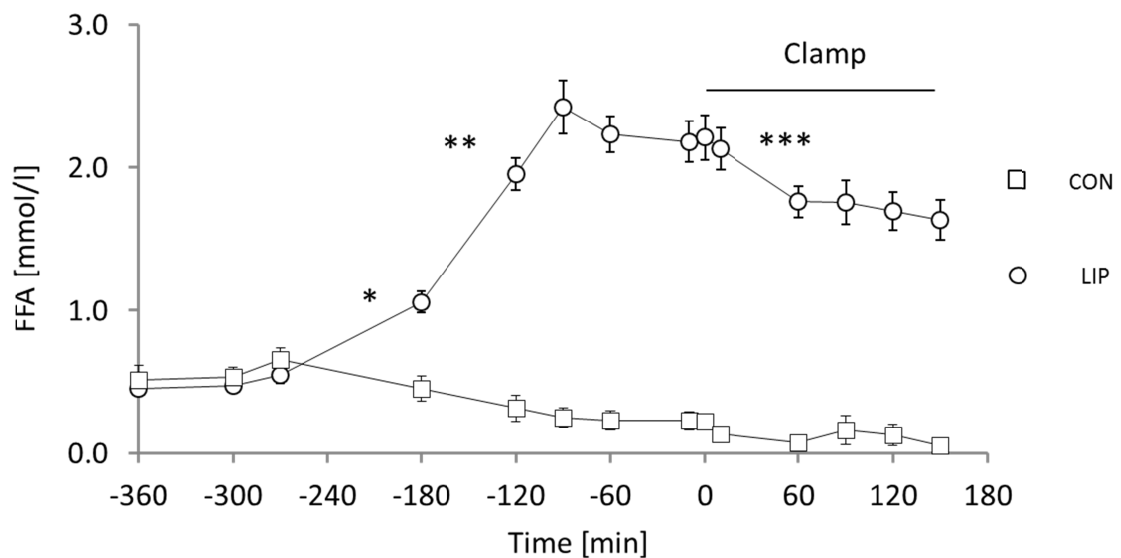


Figure 5. Plasma free fatty acids (FFA-IR group) Plasma FFA levels during glycerol/control-group [CON (squares, n = 7)] and during lipid [LIP (circles, n = 16)] infusion (-240 until +150 min) and during the hyperinsulinemic-euglycemic clamp (0 until +150 min) in lean, healthy, young humans. Data are means \pm SEM. $*p < 10^{-6}$ (LIP -270 min vs. -180 min); $**p < 10^{-6}$ (LIP -180 min vs. -60 min); $***p < 0.0003$ (LIP -60 min vs. +150 min); $p < 0.0005$ (CON -270 min vs. +150 min); $p < 10^{-6}$ (LIP vs. CON +150 min).

After 90 min lipid infusion the TAG concentration constantly increased, with an increase of about 190% from -270 min up to +150 min ($*p < 10^{-7}$). The TAG concentration during the glycerol infusion remained almost constant ($**p < 0.073$). Of note is that after starting with comparable values at -360 min the increase of the lipid graph at +150 min is nearly fourfold to the glycerol ($p < 10^{-6}$) (**Figure 6**).

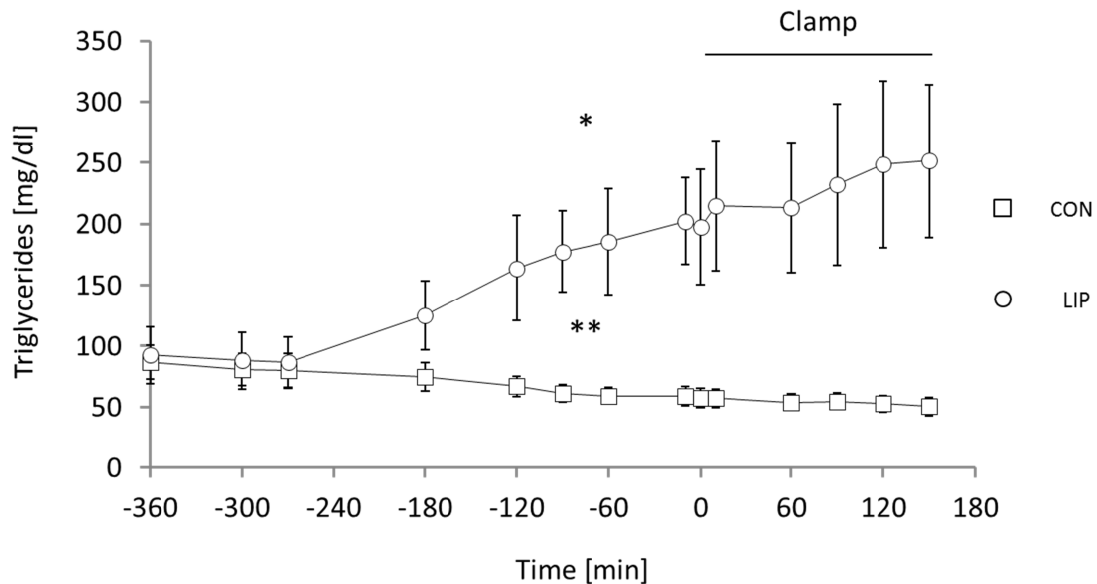


Figure 6. Plasma triglycerides (FFA-IR group) Plasma TG levels during glycerol (squares, $n = 7$) and during lipid (circles, $n = 16$) infusion (-240 until +150 min) and during the hyperinsulinemic-euglycemic clamp (0 until +150 min) in lean, healthy, young humans. Data are means \pm SEM. $*p < 10^{-7}$ (LIP -270 min vs. +150 min); $**p < 0.073$ (CON -270 min vs. +150 min); $p < 10^{-6}$ (LIP vs. CON +150 min).

While lipid infusion was given glycerol concentration slightly increased during the first 4 h with one exception after 5 h. After starting clamp the glycerol concentration decreased ($*p < 10^{-7}$). The glycerol concentration during the glycerol infusion was almost constant of a mean value of 30.65 [g/l] ($p < 0.19$) (**Figure 7**). After 9 h lipid or glycerol infusion a difference of $**p < 10^{-4}$ was to be seen.

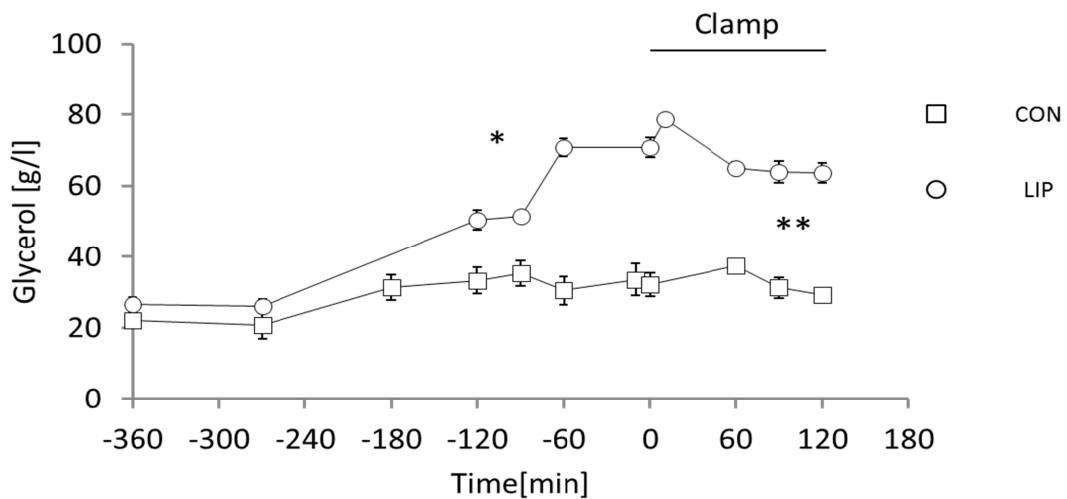


Figure 7. Plasma glycerol (FFA-IR group) Plasma glycerol levels during glycerol (squares, n = 7) and during lipid (circles, n = 16) infusion (-240 until +150 min) and during the hyperinsulinemic-euglycemic clamp (0 until +150 min) in lean, healthy, young humans. Data are means \pm SEM. * $p < 10^{-7}$ (LIP -270 min vs. +150 min); $p < 0.19$ (CON -270 vs. +150 min); ** $p < 10^{-4}$ (LIP vs. CON +150 min).

During lipid infusion, plasma insulin levels increased after starting hyperinsulinemic-euglycemic clamp about 538% (LIP * $p < 10^{-5}$); during glycerol infusion about 328%. (Figure 8). During the clamp the values did not change (** $p < 0.22$).

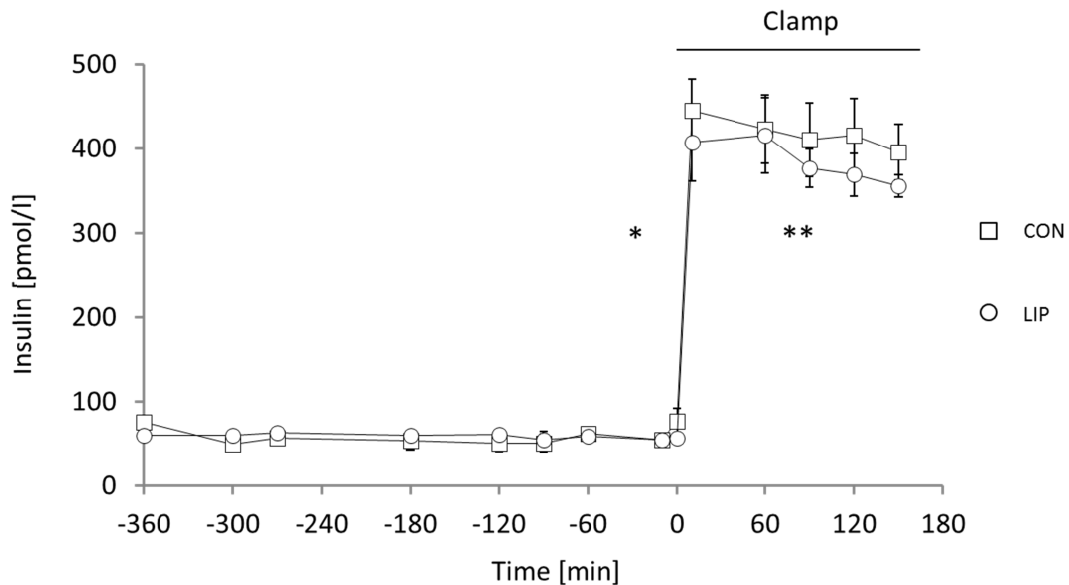


Figure 8. Plasma insulin (FFA-IR group) Plasma insulin levels during glycerol (squares, n = 16) and during lipid (circles, n = 7) infusion (-240 until +150 min) and during the hyperinsulinemic-euglycemic clamp (0 until +150 min) in lean, healthy, young humans. Data are means \pm SEM. * $p < 10^{-5}$ (LIP 0 min vs. +30 min); ** $p < 0.22$ (LIP +30 min vs. +150 min); $p < 0.0001$ (CON 0 min vs. +30 min); $p < 0.035$ (CON +30 min vs. +150 min); $p < 0.177$ (LIP vs. CON +150 min).

During first 3 h the C-peptides concentration decreased similarly in both infusions [$*p < 10^{-7}$ (LIP -270 min vs. -180 min); $*p < 10^{-4}$ (CON -270 min vs. -180 min)] (**Figure 9**).

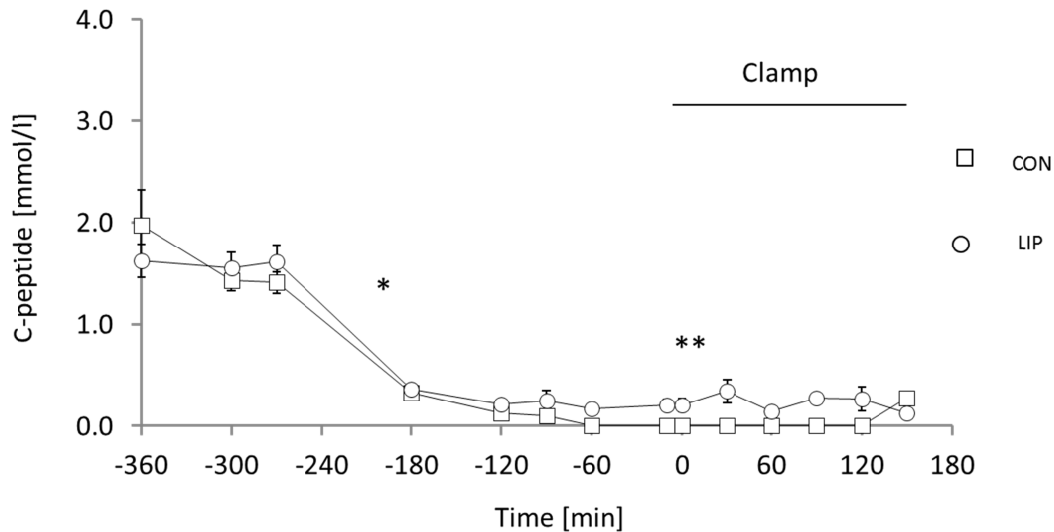


Figure 9. Plasma C-peptides (FFA-IR group) Plasma C-peptide levels during glycerol (squares, $n = 7$) and during lipid (circles, $n = 16$) infusion (-240 until +150 min) and during the hyperinsulinemic-euglycemic clamp (0 until +150 min) in lean, healthy, young humans. Data are means \pm SEM. $*p < 10^{-7}$ (LIP -270 min vs. -180 min); $**p < 0.08$ (LIP -180 min vs. +150 min); $p* < 10^{-4}$ (CON -270 min vs. -180 min).

4.1.2 Whole-body glucose metabolism

Whole-body glucose disposal in 16 lean healthy young humans after 4 h lipid and glycerol infusion; compared to control conditions glucose disposal was reduced by 64% during lipid infusion ($*p < 10^{-5}$) (**Figure 10**).

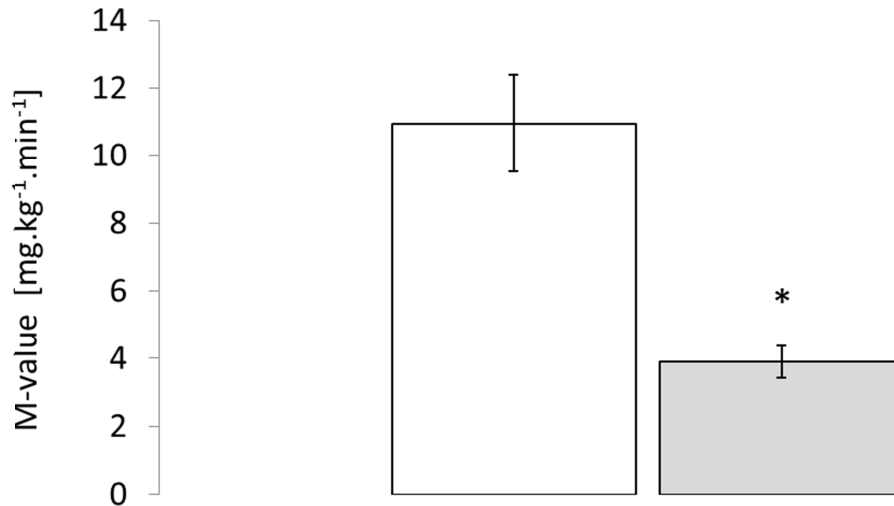


Figure 10. Whole-body glucose disposal (unpaired) Whole-body glucose disposal in lean, healthy, young humans after 4 h glycerol infusion (CON white column, n = 7), after 4 h lipid infusion (LIP grey column, n = 16). Data are means \pm SEM. * $p < 10^{-5}$ vs. control-group and a reduction about 64%.

4.1.2.1 Analysis of gender effects on M-value

The gender-related whole-body-glucose disposal of the FFA-IR group and insulin signalling group were examined (**Figure 11**). All data were taken of the volunteers of both study groups; data were taken unpaired. The whole-body glucose disposal was measured of 8 women and 15 men during lipid and glycerol infusion. Glycerol infusion was taken as control condition. Female glucose disposal was reduced compared to the CON by 43.7% during lipid infusion (* $p = 0.02$). Glucose disposal of male volunteers was reduced by 65.3% (** $p < 10^{-5}$). Additionally the BSA-value (**Figure 12**) was measured. Men had an average-value of 1.97 m² and women of 1.7 m² (reduced about 13.7%). There was no significant gender-related difference of the whole-body-glucose disposal during the lipid infusion.

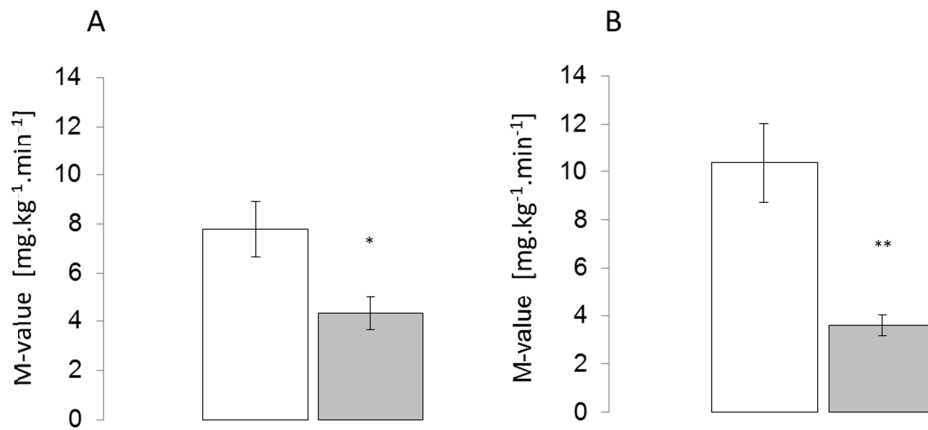


Figure 11. Analysis of gender effect (unpaired) Whole-body glucose disposal in lean healthy young humans according to gender, female (A) and male (B) after 4 h glycerol infusion. Female (CON white column, n = 7; LIP grey column, n = 8) and male (CON white column, n = 7; LIP grey column, n = 15). Data are means ± SEM. Female *p = 0.02 and a reduction of 43.7% vs. control-group and male **p < 10⁻⁵ and a reduction of 65.3% vs. control-group.

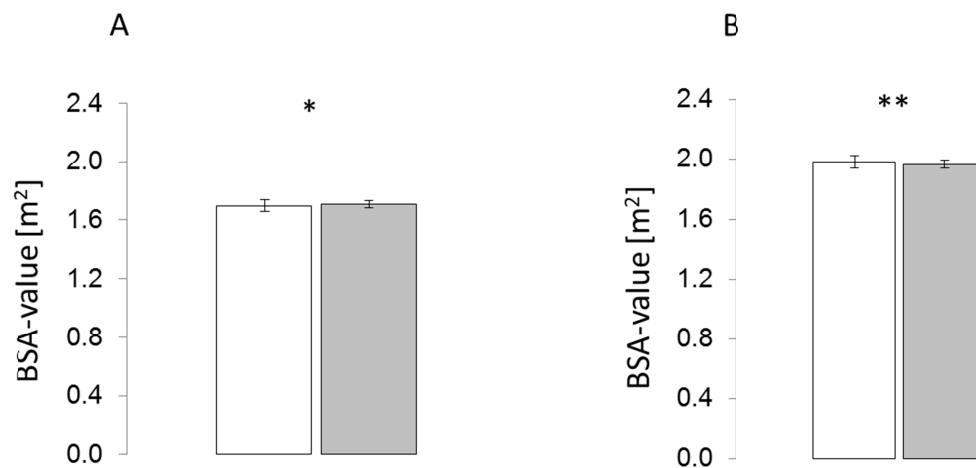


Figure 12. Analysis of gender effect on BSA-value (unpaired) BSA measured of lean healthy young humans according to gender, female (A) and male (B) after 4 h glycerol infusion. Female (CON white column, n = 7; LIP grey column, n = 8) and male (CON white column, n = 7; LIP grey column, n = 15). Data are means ± SEM. Female *p < 0.86 vs. control-group and male **p < 0.51 vs. control-group.

4.1.2.2 Analysis of gender effects on M-value

We examined a gender-related difference of the whole-body glucose disposal under paired conditions of the FFA-IR group and insulin signalling group [the volunteers participated in both experimental dates of both studies (lipid and glycerol infusion)]. The whole-body glucose disposal was measured of 7 women and 7 men during lipid and glycerol infusion. Glycerol infusion was taken as control condition (**Figure 13**). The

whole-body glucose disposal was reduced of both genders compared to control conditions. Female glucose disposal was reduced compared to the control conditions by 42% during triglyceride rich infusion (*p = 0.005). Male glucose disposal had a reduction of 53% (**p = 0.003) too. The average BSA-value was comparable to unpaired conditions (Figure 14). There was no significant gender-related difference of the whole-body glucose disposal during the lipid infusion.

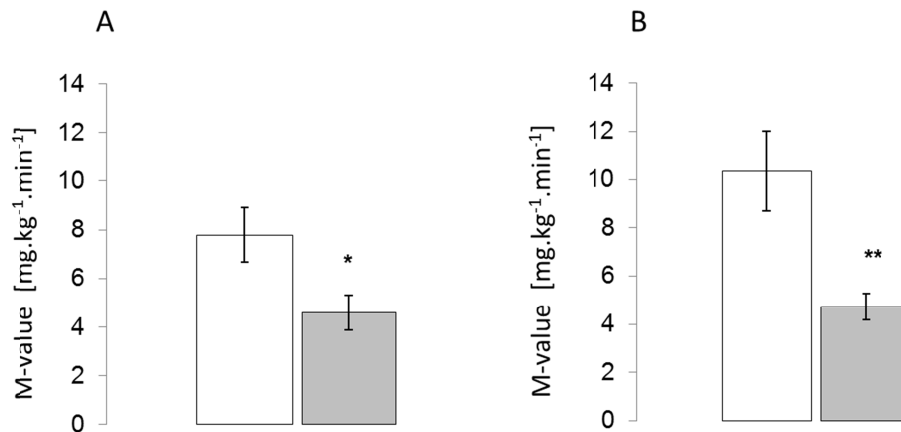


Figure 13. Analysis of gender effect (paired) Whole-body glucose disposal in lean healthy young humans (paired) according to gender, female (A) and male (B), after 4 h glycerol infusion. Female (CON white column, n = 7; LIP black column, n = 7) and male (CON white column, n = 7; LIP black column, n = 7). Data are means ± SEM. Female *p = 0.005 and a reduction about 42% vs. control-group and male **p = 0.003 and a reduction about 53% vs. control-group.

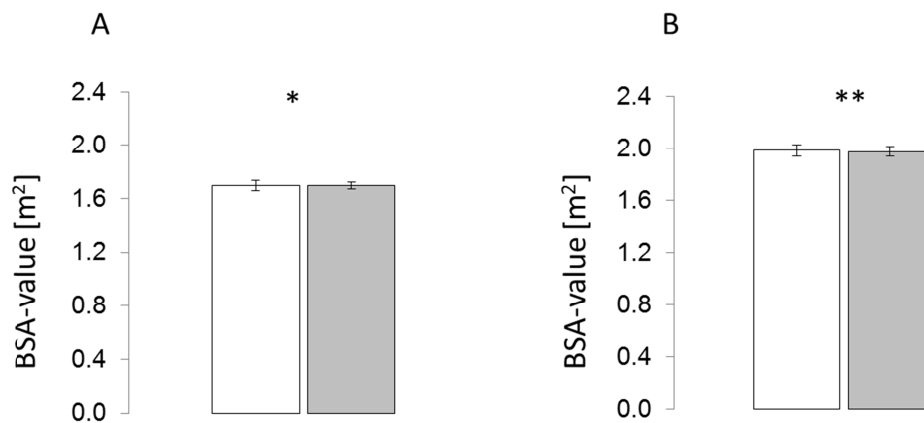


Figure 14. Analysis of gender effect on BSA-value (paired) BSA value (m²) measured of lean young healthy humans (paired) according to gender, female (A) and male (B), after 4 h glycerol infusion. Female (CON white column, n = 7; LIP black column, n = 7) and male (CON white column, n = 7; LIP black column, n = 7). Data are means ± SEM. Female *p < 0.86 vs. control-group and male **p < 0.51 vs. control-group.

4.1.3 Myocellular lipid intermediates

4.1.3.1 Diacylglycerol

The DAG concentration under paired conditions was examined. DAG in the cytosol fraction tended to be higher during lipid infusion than during glycerol infusion after 2.5 h ($p < 0.05$). DAG concentrations in both fractions did not change during glycerol infusion, but tended to increase after 2.5 h in the cytosol fraction ($p = 0.06$ vs. basal) and in the membrane fraction ($*p = 0.04$ vs. basal), decreased in the cytosol fraction ($**p = 0.04$, 2.5 h vs. 4 h) and tended to decrease in the membrane fraction ($p = 0.11$, 2.5 h vs. 4 h lipid infusion) but tended to remain increased compared to basal concentrations after 4 h in the cytosol fraction ($p = 0.22$ vs. basal) and in the membrane fraction ($p = 0.15$ vs. basal) (**Figure 15**).

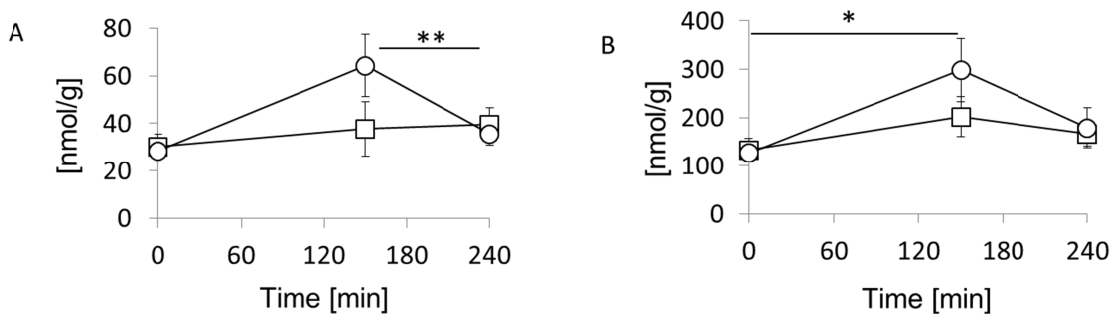


Figure 15. DAG cytosolic and membrane (paired) DAG concentrations in the cytosolic fraction (A) and DAG concentration in the membrane fraction (B) during glycerol infusion (squares, $n = 16$) and during lipid infusion (circles, $n = 7$). Data given as mean \pm SEM. $*p = 0.04$ vs. basal and $**p = 0.04$, 2.5 h vs. 4 h.

4.1.3.2 Cytosolic diacylglycerol species

To examine which DAG species were involved and might have played a predominate role, the DAG species palmitate (P) [$C_{16}H_{32}O_2$], stearate (S) [$C_{18}H_{36}O_2$], linoleate (L) [$C_{18}H_{32}O_2$], arachidonate (A) [$C_{20}H_{32}O_2$] and oleate (O) [$C_{18}H_{34}O_2$] were analysed. The species were measured in the cytosol and membrane fraction.

DAG species in the cytosol fraction tended to be higher in the species palmitate/oleate (PO) $p < 0.005$, oleate (OO) $p < 0.005$, oleate/linoleate (OL) $p < 10^{-5}$ and linoleate (LL) $p < 10^{-7}$. Also in the membrane fraction it became apparent that the same species were

predominant: OO $p < 0.005$, LL $p < 10^{-6}$ and palmitate/ linoleate (PL) $p < 0.005$ (**Figure 16**).

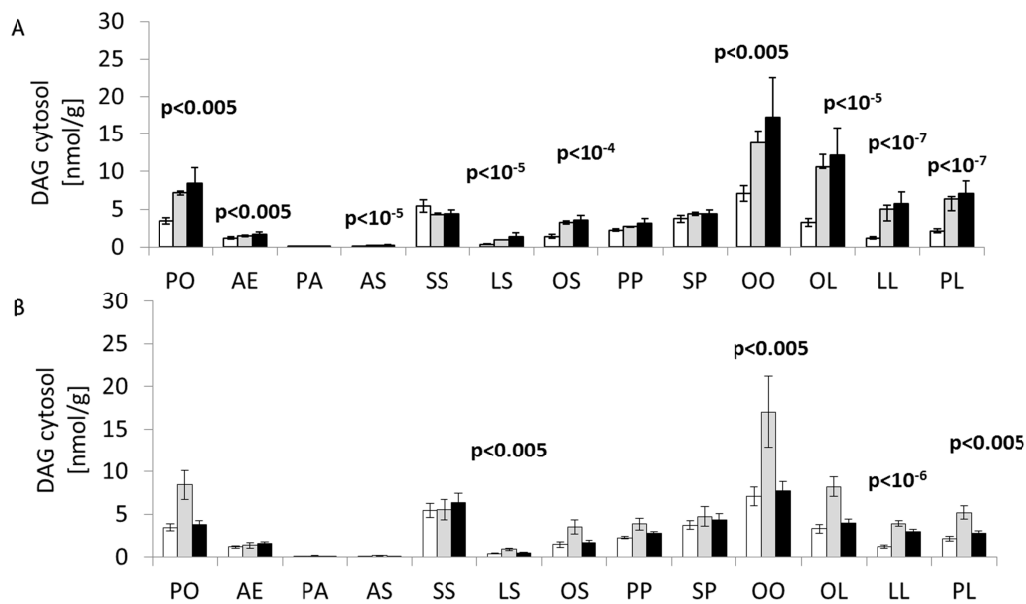


Figure 16. Cytosolic DAG species (A) Cytosol fraction of myocellular DAG species concentrations in young healthy lean humans (CON, white columns, $n = 16$), [obese (OB), dark grey columns, $n = 5$] and in elderly obese patients with type 2 diabetes (T2DM, black columns, $n = 4$). (B) Cytosol fraction of myocellular DAG species concentrations in CON at baseline (white columns, $n = 16$), after 2.5 h lipid infusion (dark grey columns, $n = 12$) and after 4 h lipid infusion (black columns, $n = 16$). Data are means \pm SEM.

4.1.3.3 Membrane diacylglycerol species

DAG species in the cytosol fraction tended to be higher in the species palmitate/linoleate (PL) $p < 10^{-4}$, linoleate (LL) $p < 10^{-6}$ and palmitate/arachidonate (PA) $p < 0.005$ and arachidonate/stearate (AS) $p < 0.005$. In the membrane fraction the same species were still predominant: oleate/linoleate (OL) $p < 0.005$, linoleate/linoleate (LL) $p < 10^{-6}$ and palmitate/linoleate (PL) $p < 0.005$ (**Figure 17**).

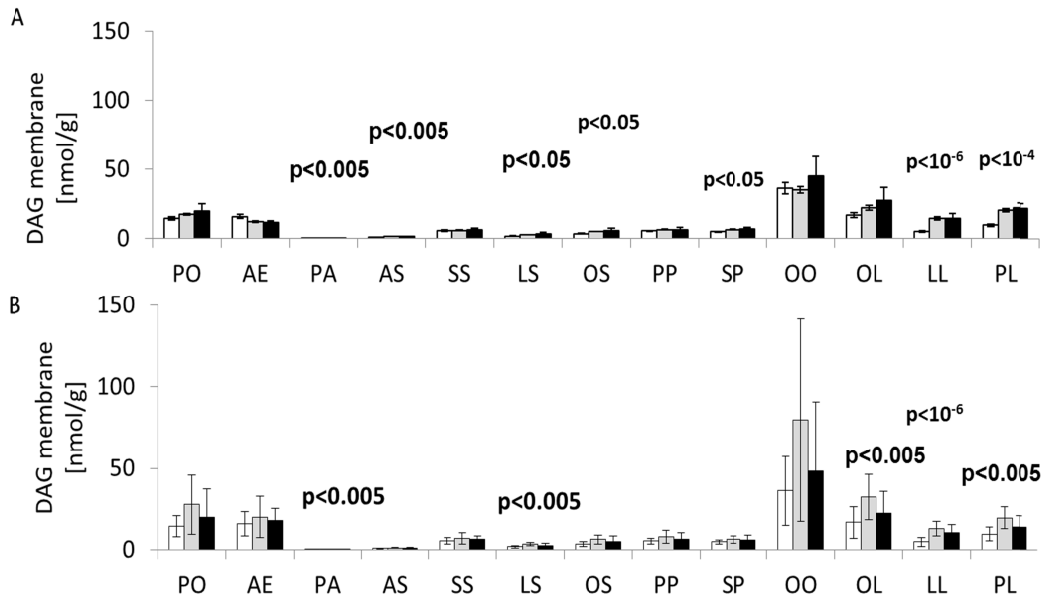


Figure 17. Membrane DAG species (A) Membrane fraction of myocellular DAG species concentrations in young healthy lean humans (CON, white columns, n = 16), (OB, dark grey columns, n = 5) and in elderly obese patients with type 2 diabetes (T2DM, black columns, n = 4). (B) Membrane fraction of myocellular DAG species concentrations in CON at baseline (white columns, n = 16), after 2.5 h lipid infusion (dark grey columns, n = 12) and after 4 h lipid infusion (black columns, n = 16). Data are means \pm SEM.

4.1.3.4 Ceramides

The myocellular ceramides concentration was not significantly increased or suppressed during the glycerol and triglyceride rich infusion (**Figure 18**).

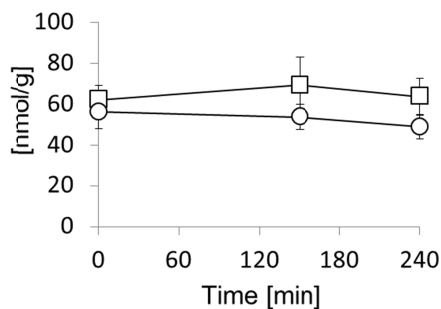


Figure 18. Myocellular ceramides (paired) Myocellular ceramides concentrations during glycerol infusion (squares) and during lipid infusion (circles). Data given as mean \pm SEM.

4.1.4 Myocellular protein kinase C

Activation of PKC isoforms did not change during glycerol infusion in all isoforms. Activation of PKC θ tended to increase after 4 h lipid infusion ($p = 0.07$ vs. basal). Activation of PKC β increased after 4 h lipid infusion compared to 2.5 h lipid infusion ($p = 0.02$ 4 h vs. 2.5 h lipid infusion) (**Figure 19**).

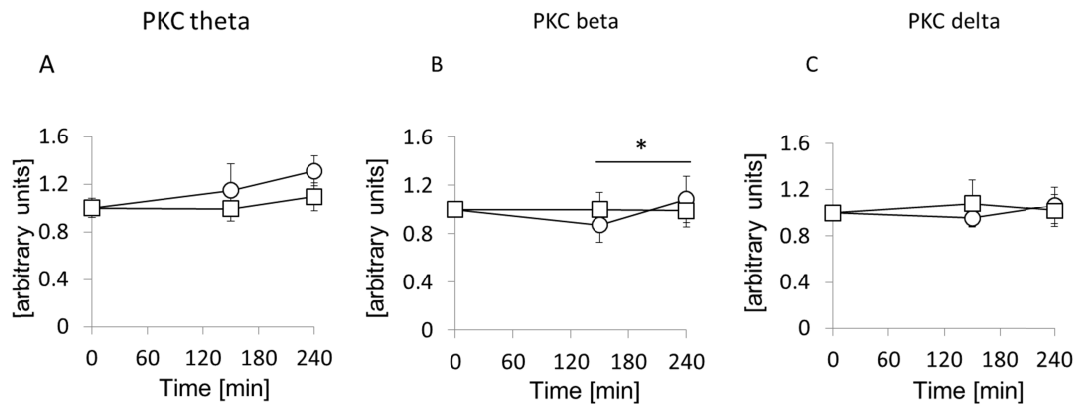


Figure 19. PKC (paired) Relative membrane to cytosol fraction relative to basal fraction (= 1) referred to as activation of PKC θ (A), β (B) and δ (C). PKC concentration during glycerol infusion (squares) and during lipid infusion (circles). Data given as mean \pm SEM.

4.2 Insulin signalling group

The plasma values of the volunteers were measured once during lipid infusion and secondly during glycerol infusion (**Figure 4**) to examine the lipid induced insulin resistance. The glycerol infusion served as control (CON). Results are shown in following figures (**Figures 20 - 26**).

4.2.1 Plasma metabolites

Young healthy lean humans were given lipid infusion [(LIP) $n = 7$] and at a later date glycerol infusion [(CON) $n = 7$] over 9 h. FFA concentration during the lipid infusion increased during the first 4 h ($*p < 10^{-5}$) and after hyperinsulinemic-euglycemic clamp decreased slightly ($**p < 0.0014$). During the glycerol infusion the FFA concentration remained almost constant ($p = 0.57$) (**Figure 20**).

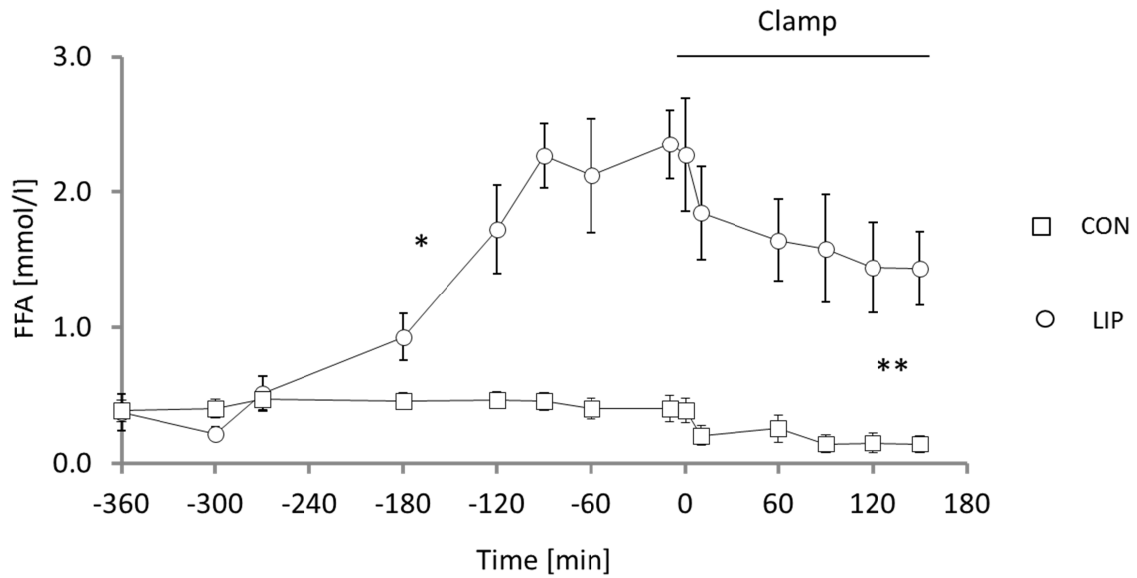


Figure 20. Plasma free fatty acids (insulin signalling group) Plasma FFA levels during glycerol (squares, n = 7) and during lipid (circles, n = 7) infusion (-240 until +150 min) and during the hyperinsulinemic-euglycemic clamp (0 until +150 min) in lean, healthy, young humans. Data are means \pm SEM. * $p < 10^{-5}$ (LIP -270 min vs. -90 min); ** $p < 0.0014$ (LIP 0 min vs. +150 min); $p < 0.0007$ (CON 0 min vs. +150 min); $p < 10^{-4}$ (LIP vs. CON +150 min).

After 2 h lipid infusion TAG concentration increased constantly (* $p < 0.0007$), whereas the TAG concentration during the glycerol infusion remained almost constant (**Figure 21**). The course of the two graphs after +150 min has a difference of ** $p < 0.002$.

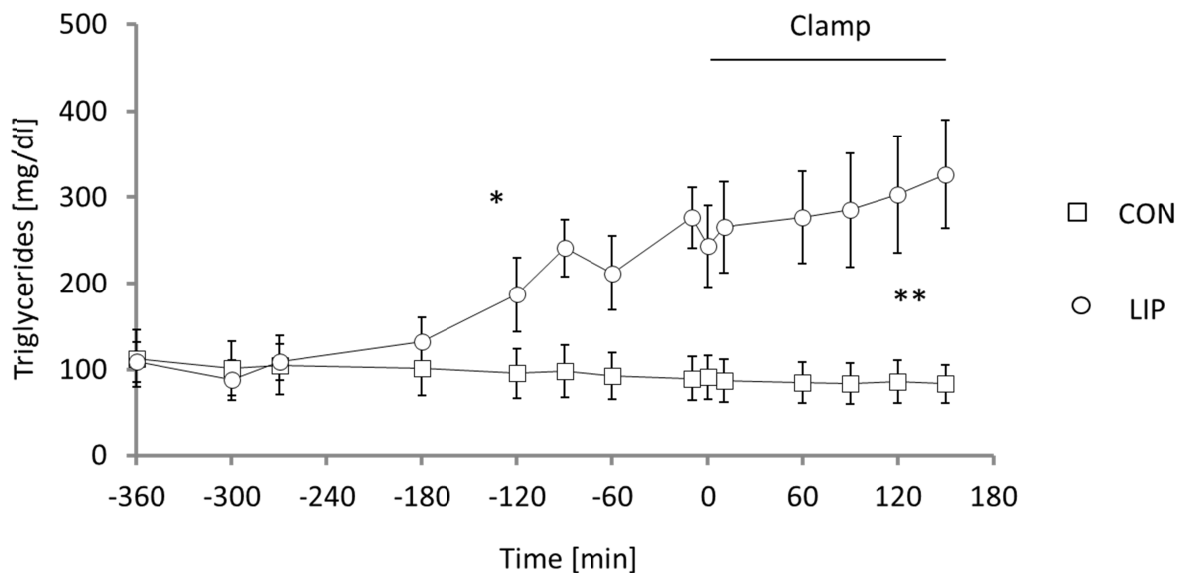


Figure 21. Plasma triglycerides (insulin signalling group) Plasma triglyceride levels during glycerol (squares, n = 7) and during lipid (circles, n = 7) infusion (-240 until +150 min) and during the hyperinsulinemic-euglycemic clamp (0 until +150 min) in lean, healthy, young humans. Data are means \pm SEM. * $p < 0.0007$ (LIP -270 min vs. +150 min); ** $p < 0.002$ (LIP vs. CON +150 min).

After starting hyperinsulinemic-euglycemic clamp the glycerol concentration constantly decreased. The reduced peak at 90 min is influenced by a statistical outlier of one participant about 18.2 g/l in comparison to the mean of 50.2 g/l. The glycerol concentration during the glycerol infusion was almost constant (**p < 0.06), with no great different value in comparison to the lipid graph after +150 min (*p < 0.18) (**Figure 22**).

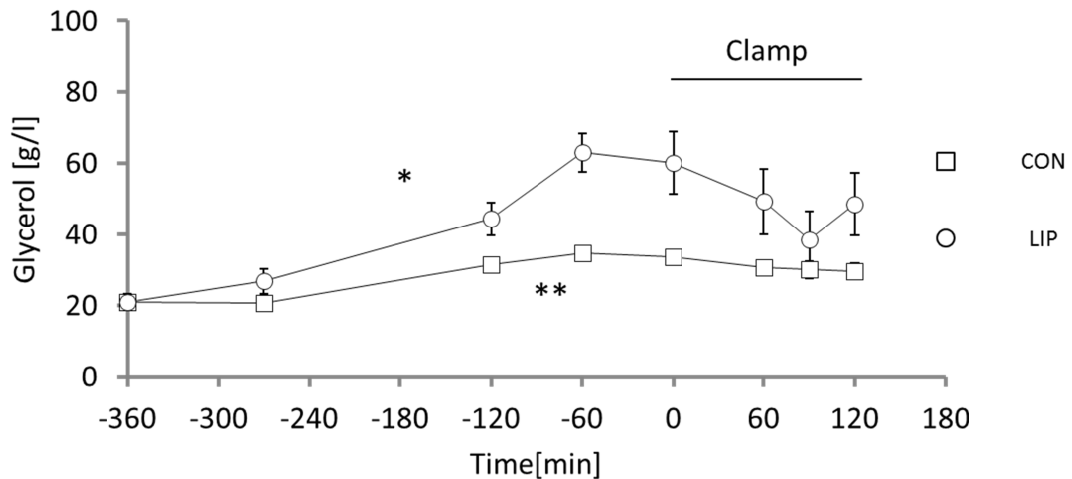


Figure 22. Plasma glycerol (insulin signalling group) Plasma glycerol levels during glycerol (squares, n = 7) and during lipid (circles, n = 7) infusion (-240 until +150 min) and during the hyperinsulinemic-euglycemic clamp (0 until +150 min) in lean, healthy, young humans. Data are means \pm SEM. *p < 0.18 (LIP vs. CON +150 min); **p < 0.06 (CON -270 min vs. +150 min).

During lipid (LIP) infusion plasma insulin levels increased after starting hyperinsulinemic-euglycemic clamp about 388% (LIP *p < 10^{-6}); during glycerol infusion about 363% (p < 10^{-4}) (**Figure 23**). During the clamp the graph did not change (**p < 0.32).

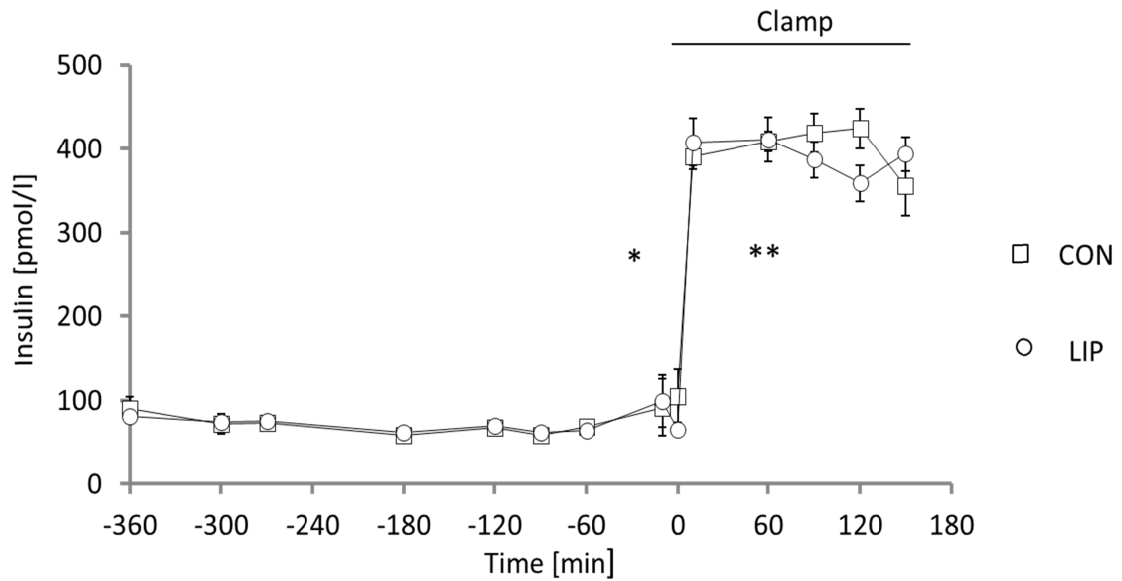


Figure 23. Plasma insulin (insulin signalling group) Plasma insulin levels during glycerol (squares, n = 7) and during lipid (circles, n = 7) infusion (-240 until +150 min) and during the hyperinsulinemic-euglycemic clamp (0 until +150 min) in lean, healthy, young humans. Data are means \pm SEM. * $p < 10^{-6}$ (LIP 0 min vs. +30 min); ** $p < 0.32$ (LIP +30 min vs. +150 min); $p < 10^{-4}$ (CON 0 min vs. +30 min).

During first 3 h the C-peptide concentration decreased during lipid (* $p < 10^{-6}$) and glycerol infusion ($p < 0.004$) and then remained nearly constant [** $p < 0.22$ (LIP -180 min vs. +150 min)] (**Figure 24**).

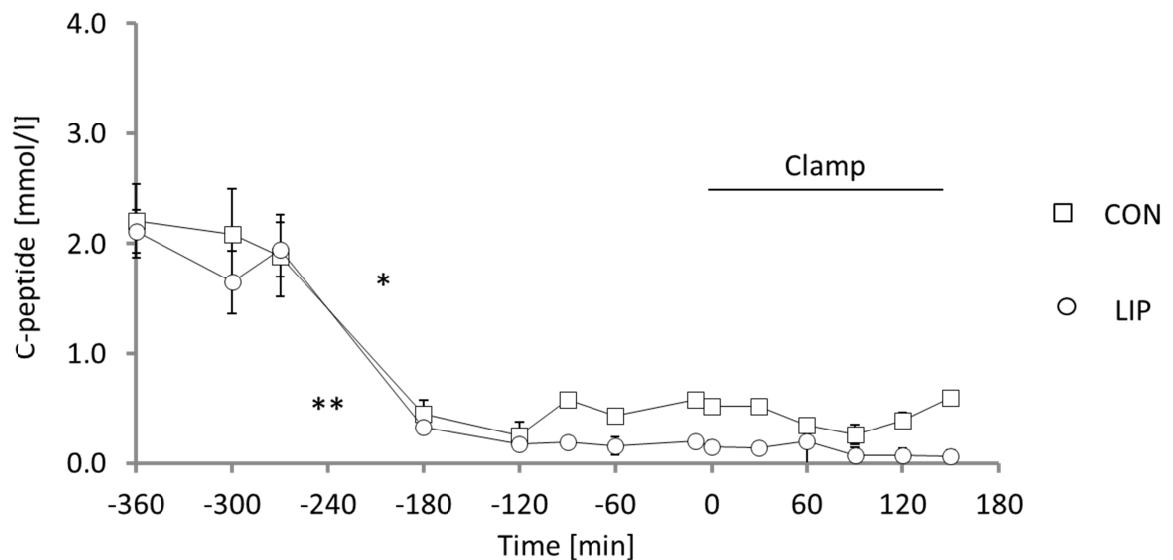


Figure 24. Plasma C-peptides (insulin signalling group) Plasma C-peptide levels during glycerol (squares, n = 7) and during lipid (circles, n = 7) infusion (-240 until +150 min) and during the hyperinsulinemic-euglycemic clamp (0 until +150 min) in lean, healthy, young humans. Data are means \pm SEM. * $p < 10^{-6}$ (LIP -270 min vs. -180 min); ** $p < 0.22$ (LIP -180 min vs. +150 min); $p < 0.004$ (CON -270 min vs. -180 min); $p < 0.01$ (LIP vs. CON +150 min).

4.2.2 Endogenous glucose production

The EGP of volunteers of FFA-IR- and insulin signalling group was measured. The EGP was decreased ($*p < 10^{-7}$) during lipid infusion after starting the hyperinsulinemic-euglycemic clamp. The basal EGP was comparable during lipid and glycerol infusion (**Figure 25**).

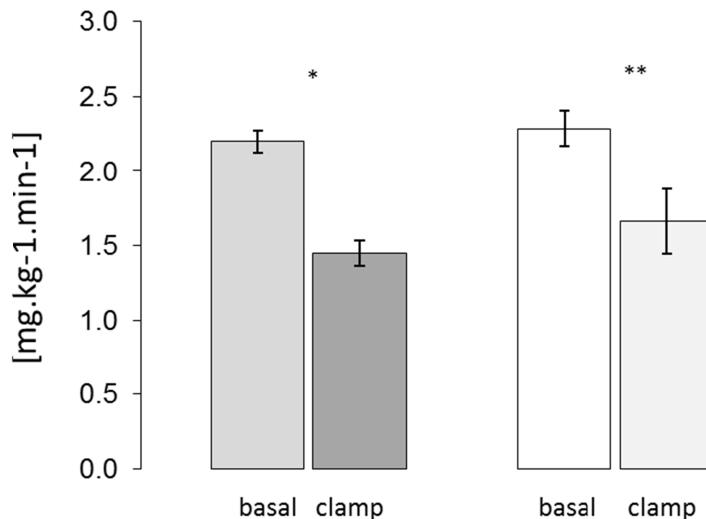


Figure 25. Endogenous glucose production Left columns: lipid (light grey column: basal, dark grey column: clamp), right columns: glycerol (white column; basal, light grey column: clamp). $*p < 10^{-7}$, $**p = 0.09$. Data are means \pm SEM.

4.2.3 Analysis of gender effects on EGP

The gender-related EGP of volunteers of FFA-IR and insulin signalling groups were examined (**Figure 26**). All data were taken of the volunteers of both study groups; data were taken unpaired. The whole-body glucose disposal was measured of 8 women and 15 men during lipid and glycerol infusion. Neither the basal nor the suppressed EGP significantly differed between men and women during lipid and glycerol infusion.

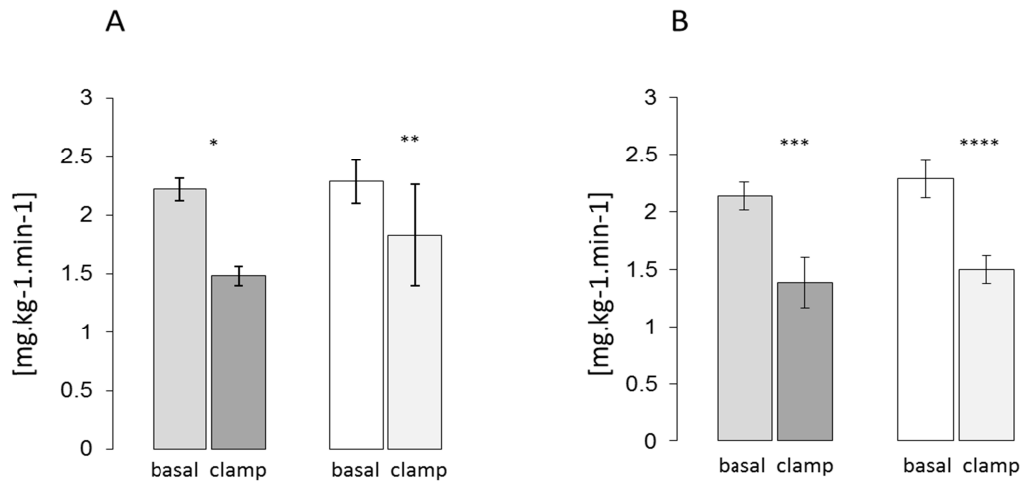


Figure 26. Endogenous glucose production gender-related (A) male: left columns: lipid (light grey column: basal, dark grey column: clamp), right columns: glycerol (white column: basal, light grey column: clamp). (B) female: left columns: lipid (light grey column: basal, dark grey column: clamp), right columns: glycerol (white column: basal, light grey column: clamp). * $p < 10^{-5}$; ** $p < 0.029$; *** $p < 0.031$; **** $p < 0.0009$. Data are means \pm SEM.

5. Discussion

The results briefly summarised: the present study revealed short term elevation of plasma FFA, caused by intralipids, resulting in an increase of myocellular contents of DAG. The DAG concentrations in the membrane and cytosol fractions did not change during glycerol infusion but increased after 2.5 h ($p < 0.05$). The increase of myocellular DAG was followed by PKC activation at 4 h. The ceramides concentration did not change significantly during the glycerol or triglyceride rich infusion. Thus, the DAG stimulated the activity of PKC θ and induced the muscular insulin resistance. Especially DAG isoforms e.g. palmitate and linoleate are of interest in the pathway of the lipid induced insulin resistance. In the membrane and cytosol fraction the DAG species palmitate and linoleate were apparent ($p < 0.05$). Further the whole-body glucose disposal was measured during lipid infusion. It was reduced by 64% during lipid infusion ($*p < 10^{-5}$). The volunteers were divided into male and female cohorts to examine if the whole-body glucose-disposal had a gender relation. No significant gender-related difference was revealed.

5.1 Effect of gender on whole-body glucose disposal and EGP

The EGP is regulated by plasma glucose and insulin concentration. Previous studies examined that in the presence of basal insulin concentration, an increase in plasma glucose concentration is based on a decreased EGP [78]. It is to be discussed if a gender determines or partly influences the cause of the whole-body glucose disposal and EGP. Several human and animal studies revealed controversial results. In obese the whole-body insulin sensitivity was as well as non-oxidative glucose disposal higher in females compared to males during both lipid and saline infusion ($p < 0.001$ and $p = 0.01$) [79]. Homko et al. 2003 related of a female lipid induced reduction in insulin-mediated glucose uptake [80]. Further, Frias et al. 2001 revealed a gender dependant difference that lean females have no inhibited insulin-stimulated glucose disposal in contrast to males [81]. The non-oxidative glucose R_d was decreased by 15% in men and was not significantly affected in women and the basal EGP was unaffected by elevation of plasma non-esterified fatty acids [81]. Vistisen et al. asserted that the results were caused by the deficiency in the examination of non-oxidative glucose disposal in 11 men [79]. An animal study examined a sex dependant difference in rat hepatic lipid accumulation and insulin sensitivity in response to diet-induced obesity [82]. Females had a better insulin sensi-

tivity [79, 82-84], and in response to dietary exhibited an increased body mass and adiposity and liver fat accumulation than males by a maintained better glucose tolerance [82]. A further animal study revealed that hyperinsulinemia and insulin resistance might be associated with hypertension in male rats [84]. A gender relation is still of interest for further research.

The whole-body glucose disposal of lean healthy young humans in our study revealed no significant gender dependant difference during lipid infusion. It seems that an increase of plasma FFA leading to insulin resistance is not affected by gender. Even if the body weight increases, the whole-body glucose disposal seems to be still not related to gender [79]. Thus, lipid-induced inhibition of glucose disposal of obese [79] and lean females and males might be comparable. But these results are in contrast to Hoeg et al., who determined that after lipid rich infusion the whole-body glucose disposal was reduced by about 26% in women and about 38% in men ($p < 0.05$) [85]. Further, that after lipid infusion the insulin stimulated leg glucose uptake was reduced by about 45% in women and 60% in men [85]. According to Hoeg et al. an intralipid infusion may cause less insulin resistance of muscle glucose uptake in women than in men. On the other hand gender may not affect the relationship between liver fat and serum triglycerides [86]. Women and men have similar amounts of intra-abdominal fat but women have twice as much subcutaneous fat as men [86]. This suggests that liver fat is more proximal correlated to insulin resistance than intra-abdominal fat [86]. Although we did not examine a gender related research of muscle ceramides, TAG and DAG content, it is of interest that Vistisen et al. measured no significant gender-related difference between these. Even during the clamp it remained unchanged [79]. Therefore no gender-related preference to insulin resistance seems to exist but further examinations are necessary to confirm our results.

5.2 Effect of FFA on intracellular lipid intermediates

The present study revealed short term elevation of plasma FFA, caused by intralipids, resulting in an increase of myocellular contents of DAG. The ceramides concentration did not change significantly during the glycerol or triglyceride rich infusion. Randle et al. [60, 87] were the first to suggest in 1963 that an elevated availability of FFA had a primary role in the development of muscle insulin resistance. The thesis was based upon

observation of increasing plasma concentration of FFA in combination with diabetes and other disorders of carbohydrate metabolism [88]. The elevation of plasma FFA concentration is known to induce skeletal muscle insulin resistance by reducing glucose transport/ -phosphorylation, glycogen synthesis and glucose oxidation [53]. The accumulation of ectopic lipids (intramyocellular and hepatocellular lipids, IMCL, HCL) [4, 9, 58, 59] DAG and ceramides [53] is often a grade of the insulin resistance. This assumption is supported in human and animal studies [89]. The hypothesis is to be established if the triglycerides are inert [59, 62]. Additionally if the lipid metabolites DAG and ceramides inhibit the signalling and whether the myocellular ceramides and ceramidase activity are the primary culprits [90]. The DAG was significantly increased after 2.5 h, whereas the ceramides did not differ. In contrast to Summers et al., who proposed ceramides as the “primary culprits” [64, 90] and Adams et al. [91], whose study reported of an increase of ceramides similarly to the obese subjects; the muscle ceramides content was significantly correlated with the plasma free fatty acid concentration or respectively particularly contributed to subsequent metabolic complications [50, 92]. Adams et al. [91] suggested that obesity is associated with increased intramyocellular ceramides content [91]. Consitt et al. referred in his review of controversial studies [93], reporting both of an elevated amount of ceramides in the skeletal muscle of insulin resistant animals [93], lipid infused humans [94], obese, insulin-resistant humans [91], lean offspring of T2DM and of no examined differences in ceramides levels between lean and obese individuals with similar insulin sensitivity [93, 95]. According to our results, in comparison to the controversial study reports [96], Summers [90] considered that ceramides participate but have not a primary role in impairing the insulin signalling [97]. The DAGs seem to determine the primary role [98]. Kumashiro et al. described DAG as the best predictor of insulin resistance [74] and DAGs could be more related to skeletal muscle insulin resistance in humans as previously thought. The impairment in the post receptor insulin signalling pathway seems to be central in the development of the fatty acid insulin resistance [99] and it has to be evaluated if the localisation of DAG and which kind of molecular species of DAG are preferentially related to insulin resistance in human skeletal muscle.

It is to be considered, which DAG species and where localized (membrane or cytosol) have a predominant role in the insulin signalling cascade. Bergman et al. examined in a current study if all DAG molecular species were equally deleterious to insulin sensitivi-

ty. He determined that the majority (76 - 86%) DAG species were localised in the membrane fraction and there were no significant differences in cytoplasmic DAG species ($p > 0.12$) [100]. Of the sixteen measurable membrane DAG species especially, di-C18:0 (stearate) was significantly related to insulin sensitivity [100]. In contrast to the present study we examined a preferential role of the DAG species linoleate, oleate and palmitate in the membrane and cytosolic fraction by neglecting its position. For example palmitate was significantly found in the membrane fraction on both the first (PA $p < 0.005$; PL $p > 10^{-4}$) and second position (SP $p < 0.05$). All three species seemed to be comparably participated in the lipid-induced insulin resistance; but our results are only partly attested. Controversial studies indicated that fatty acids other than palmitate particularly linoleate could induce muscle insulin resistance [101, 102] and on the other hand linoleate, oleate and palmitate had similar inhibitory effects on glycogen synthesis [101, 103]. Alkhateeb et al. revealed that especially palmitate provoked insulin resistance in skeletal muscle by impairing insulin induced activation of Akt and PKC θ [99].

Further Bergman et al. suggested that only saturated DAG in skeletal muscle membranes were related to insulin resistance in humans [100]. On the contrary, Amati et al. [58] revealed DAG species containing one unsaturated and one saturated fatty acids were lower in obese muscle, but DAG species containing unsaturated fatty acids at both positions were higher in obese muscle. It has to be determined whether specific fatty acids, e.g. palmitate, oleate, linoleate, stearate or arachidonate stimulate DAG synthesis and if this is linked to insulin resistance [58]. It is to suggest that DAG have a relation to insulin resistance [58] and specific DAG species, especially palmitate and linoleate, might be important in lipid signalling pathway [104]. It seems that further examinations are necessary to determine and to specify the predominant role of which DAG species in the insulin signalling pathway.

In contrast to the ceramides, which have a direct inhibiting influence on IRS-1 and AKT-phosphorylation, DAG induce an insulin resistance by stimulating PKC, leading to activation of the atypical isoform PKC θ [63, 98]. We examined an increased activation of PKC θ ($p = 0.04$) compared to the isoform PKC β ($p = 0.17$) and δ ($p = 0.21$) under unpaired conditions. Whereas in the paired comparison the activation tended to in-

crease in PKC θ after 4 h lipid infusion ($p = 0.07$ vs. basal) and significantly increased in the isoform PKC β .

Several studies imply a PKC activation causes skeletal muscle insulin resistance and demonstrates an association between DAG and PKC activation (e.g. [98, 105, 106]). For example Itani et al. established that humans, after 6 h of having received a lipid heparin infusion, had a reduction of insulin stimulated glucose disposal by 43% and both skeletal muscle DAG mass and PKC activity were increased fourfold. These results are reflected in our study. PKC activation was increased after 4 h lipid infusion, whereas its activation during glycerol infusion was nearly constant. It is believed that PKC θ activation results in the serine phosphorylation of upstream molecules in the insulin signalling cascade, which subsequently inhibit this pathway [93]. Though of note is not the participation of the PKCs, but rather the time interval until activation and which kind of PKC isoform is primarily included.

Several studies were published concerning participation of PKC isoforms impairing the insulin signalling (e.g. [63, 74, 105-110]). For example Itani et al. reported in a study that when plasma FFA concentration was elevated during euglycemic clamp, the DAG mass was increased and associated with PKC isoforms especially β II and δ . There was no significant alteration in PKC θ activation [105]. Whereas in an earlier study of 2000 he reported that the membrane associated PKC β protein was elevated under basal conditions and membrane associated total PKC activity was increased under stimulated conditions in muscle of obese insulin resistant patients [107]. Especially in the liver novel isoforms as δ , ϵ , θ were examined without detecting activation of PKC θ [74]. An increased activation of PKC θ was reported in animal and human studies [62, 106, 109], whereas a present study of Erion and Shulman have found out that especially PKC isoform β II and δ are the relevant isoforms [63, 105]. The present results support the concept that DAG-induced activation of PKC θ plays a key role in causing lipid-induced insulin resistance in human skeletal muscle. Of interest is if the increased activation of PKC θ during the triglyceride rich infusion after 4 h is still higher in comparison to the isoforms β and δ by increasing the number of participants. Further examinations are needed to confirm the predominant role of the PKC isoform θ in the lipid induced insulin resistance in the skeletal muscle.

6. Conclusion

An elevation of FFA reduced whole-body insulin-stimulated glucose disposal, which was associated with an early increase of myocellular DAG at 2.5 h followed by PKC activation at 4 h, whereas the ceramides were mostly unchanged. Further no gender effect could be measured on FFA-induced insulin resistance; M-value and EGP did not differ gender-related. Subsequently the DAG stimulates the activity of PKC θ and induces the muscular insulin resistance. Especially the DAG isoforms e.g. palmitate and linoleate are of interest in the pathway of the lipid-induced insulin resistance. Skeletal muscle lipases might be of potential therapeutic interest for improving insulin resistance in obesity and T2DM.

References

1. WHO *Obesity and overweight*.
2. Harford, K.A., et al., *Fats, inflammation and insulin resistance: insights to the role of macrophage and T-cell accumulation in adipose tissue*. Proc Nutr Soc, 2011. 70(4): p. 408-17.
3. Szendroedi, J., E. Phielix, and M. Roden, *The role of mitochondria in insulin resistance and type 2 diabetes mellitus*. Nat Rev Endocrinol, 2011. 8(2): p. 92-103.
4. Badin, P.M., et al., *Altered skeletal muscle lipase expression and activity contribute to insulin resistance in humans*. Diabetes, 2011. 60(6): p. 1734-42.
5. Unger, R.H., *Minireview: weapons of lean body mass destruction: the role of ectopic lipids in the metabolic syndrome*. Endocrinology, 2003. 144(12): p. 5159-65.
6. Muoio, D.M. and P.D. Neufer, *Lipid-induced mitochondrial stress and insulin action in muscle*. Cell Metab, 2012. 15(5): p. 595-605.
7. Koves, T.R., et al., *Peroxisome proliferator-activated receptor-gamma co-activator 1alpha-mediated metabolic remodeling of skeletal myocytes mimics exercise training and reverses lipid-induced mitochondrial inefficiency*. J Biol Chem, 2005. 280(39): p. 33588-98.
8. Koves, T.R., et al., *Mitochondrial overload and incomplete fatty acid oxidation contribute to skeletal muscle insulin resistance*. Cell Metab, 2008. 7(1): p. 45-56.
9. Befroy, D.E., et al., *Impaired mitochondrial substrate oxidation in muscle of insulin-resistant offspring of type 2 diabetic patients*. Diabetes, 2007. 56(5): p. 1376-81.
10. Bruce, C.R., et al., *Endurance training in obese humans improves glucose tolerance and mitochondrial fatty acid oxidation and alters muscle lipid content*. Am J Physiol Endocrinol Metab, 2006. 291(1): p. E99-E107.
11. WHO. *Obesity and overweight, Fact sheet No. 311*. 2012; Available from: <http://www.who.int/mediacentre/factsheets/fs311/en/>.
12. Eknoyan, G., *Adolphe Quetelet (1796-1874)-the average man and indices of obesity*. Nephrol Dial Transplant, 2008. 23: p. 47-51.
13. Consultation, W.H.O.E., *Appropriate body-mass index for Asian populations and its implications for policy and intervention strategies*. Lancet, 2004. 363(9403): p. 157-63.
14. WHO. *BMI Classifications*. 07/21/2012]; Available from: http://apps.who.int/bmi/index.jsp?introPage=intro_3.html.
15. WHO. *Diabetes Fact sheet No 312*. August 2011:[Available from: <http://www.who.int/mediacentre/factsheets/fs312/en/>.
16. Florez, H. and S. Castillo-Florez, *Beyond the obesity paradox in diabetes: fitness, fatness, and mortality*. JAMA, 2012. 308(6): p. 619-20.
17. Carnethon, M.R., et al., *Association of weight status with mortality in adults with incident diabetes*. JAMA, 2012. 308(6): p. 581-90.
18. Finkelstein, E.A., et al., *Annual medical spending attributable to obesity: payer-and service-specific estimates*. Health Aff (Millwood), 2009. 28(5): p. w822-31.
19. Cawley, J. and C. Meyerhoefer, *The medical care costs of obesity: an instrumental variables approach*. J Health Econ, 2012. 31(1): p. 219-30.

20. Flegal, K.M., et al., *Prevalence of obesity and trends in the distribution of body mass index among US adults, 1999-2010*. JAMA, 2012. 307(5): p. 491-7.
21. Ogden, C.L., et al., *Prevalence of obesity and trends in body mass index among US children and adolescents, 1999-2010*. JAMA, 2012. 307(5): p. 483-90.
22. Wirth, A., *Adipositas*. 3rd ed. 2008, Heidelberg: Springer Medizin Verlag
23. Leonetti, F., et al., *Obesity, Type 2 Diabetes Mellitus, and Other Comorbidities: A Prospective Cohort Study of Laparoscopic Sleeve Gastrectomy vs Medical Treatment*. Arch Surg, 2012.
24. Julia Szendroedi, E.P.a.M.R., *Assessment of insulin sensitivity*, in *The Metabolic Syndrome*, C.D.B.a.S.H. Wild, Editor. 2011, Wiley-Blackwell: Chichester, West Sussex.
25. W.H.O. *definition and diagnosis of diabetes mellitus and intermediate hyperglycemia*. 2006; Available from: http://www.who.int/diabetes/publications/Definition%20and%20diagnosis%20of%20diabetes_new.pdf.
26. Gomez-Perez, F.J., et al., *HbA1c for the diagnosis of diabetes mellitus in a developing country. A position article*. Arch Med Res, 2010. 41(4): p. 302-8.
27. Roden, M., et al., *Rapid impairment of skeletal muscle glucose transport/phosphorylation by free fatty acids in humans*. Diabetes, 1999. 48(2): p. 358-64.
28. Roden, M. and G.I. Shulman, *Applications of NMR spectroscopy to study muscle glycogen metabolism in man*. Annu Rev Med, 1999. 50: p. 277-90.
29. (DDZ), D.D.Z. *Schwangerschaftsdiabetes (Gestationsdiabetes)*. 2005; Available from: <http://www.diabetes-heute.uni-duesseldorf.de/wasistdiabetes/index.html?TextID=1808>.
30. Perkins, J.M., et al., *Perspectives in gestational diabetes mellitus: a review of screening, diagnosis and treatment*. Clinical Diabetes, 2007. 25(2): p. 57-62.
31. Zeyda, M. and T.M. Stulnig, *Obesity, inflammation, and insulin resistance--a mini-review*. Gerontology, 2009. 55(4): p. 379-86.
32. DeFronzo, R.A., *Insulin resistance, lipotoxicity, type 2 diabetes and atherosclerosis: the missing links. The Claude Bernard Lecture 2009*. Diabetologia, 2010. 53(7): p. 1270-87.
33. Roden, M., *Muscle triglycerides and mitochondrial function: possible mechanisms for the development of type 2 diabetes*. Int J Obes (Lond), 2005. 29 Suppl 2: p. S111-5.
34. Steinbach, W.J. and R.L. Hintz, *Diabetes mellitus and profound insulin resistance in Johanson-Blizzard syndrome*. J Pediatr Endocrinol Metab, 2000. 13(9): p. 1633-6.
35. Marshall, J.D., et al., *Alstrom syndrome: genetics and clinical overview*. Curr Genomics, 2011. 12(3): p. 225-35.
36. Longo, N., Y. Wang, and M. Pasquali, *Progressive decline in insulin levels in Rabson-Mendenhall syndrome*. J Clin Endocrinol Metab, 1999. 84(8): p. 2623-9.
37. Young, J., et al., *Type A insulin resistance syndrome revealing a novel lamin A mutation*. Diabetes, 2005. 54(6): p. 1873-8.
38. Lettner, A. and M. Roden, *Ectopic fat and insulin resistance*. Curr Diab Rep, 2008. 8(3): p. 185-91.

39. Hoy, A.J., et al., *Glucose infusion causes insulin resistance in skeletal muscle of rats without changes in Akt and AS160 phosphorylation*. *Am J Physiol Endocrinol Metab*, 2007. 293(5): p. E1358-64.
40. Hager, S.R., A.L. Jochen, and R.K. Kalkhoff, *Insulin resistance in normal rats infused with glucose for 72 h*. *Am J Physiol*, 1991. 260(3 Pt 1): p. E353-62.
41. Houdali, B., et al., *Prolonged glucose infusion into conscious rats inhibits early steps in insulin signalling and induces translocation of GLUT4 and protein kinase C in skeletal muscle*. *Diabetologia*, 2002. 45(3): p. 356-68.
42. Kawanaka, K., et al., *Development of glucose-induced insulin resistance in muscle requires protein synthesis*. *J Biol Chem*, 2001. 276(23): p. 20101-7.
43. Laybutt, D.R., D.J. Chisholm, and E.W. Kraegen, *Specific adaptations in muscle and adipose tissue in response to chronic systemic glucose oversupply in rats*. *Am J Physiol*, 1997. 273(1 Pt 1): p. E1-9.
44. Wellen, K.E. and G.S. Hotamisligil, *Obesity-induced inflammatory changes in adipose tissue*. *J Clin Invest*, 2003. 112(12): p. 1785-8.
45. Cohen, J.I., L. Maayan, and A. Convit, *Preliminary evidence for obesity-associated insulin resistance in adolescents without elevations of inflammatory cytokines*. *Diabetol Metab Syndr*, 2012. 4(1): p. 26.
46. Horrillo, R., *5-Lipoxygenase activating protein signals adipose tissue inflammation and lipid dysfunction in experimental obesity*. *The journal of Immunology*, 2010. 184: p. 3978-3987.
47. Shoelson, S.E., J. Lee, and A.B. Goldfine, *Inflammation and insulin resistance*. *J Clin Invest*, 2006. 116(7): p. 1793-801.
48. Hotamisligil, G.S., N.S. Shargill, and B.M. Spiegelman, *Adipose expression of tumor necrosis factor-alpha: direct role in obesity-linked insulin resistance*. *Science*, 1993. 259(5091): p. 87-91.
49. Roden, M., *How free fatty acids inhibit glucose utilization in human skeletal muscle*. *News Physiol Sci*, 2004. 19: p. 92-6.
50. Kraegen, E.W. and G.J. Cooney, *Free fatty acids and skeletal muscle insulin resistance*. *Curr Opin Lipidol*, 2008. 19(3): p. 235-41.
51. Kelley, D.E., et al., *Dysfunction of mitochondria in human skeletal muscle in type 2 diabetes*. *Diabetes*, 2002. 51(10): p. 2944-50.
52. Szendroedi, J. and M. Roden, *Mitochondrial fitness and insulin sensitivity in humans*. *Diabetologia*, 2008. 51(12): p. 2155-67.
53. Brehm, A., et al., *Increased lipid availability impairs insulin-stimulated ATP synthesis in human skeletal muscle*. *Diabetes*, 2006. 55(1): p. 136-40.
54. Maassen, J.A., J.A. Romijn, and R.J. Heine, *Fatty acid-induced mitochondrial uncoupling in adipocytes as a key protective factor against insulin resistance and beta cell dysfunction: a new concept in the pathogenesis of obesity-associated type 2 diabetes mellitus*. *Diabetologia*, 2007. 50(10): p. 2036-41.
55. Delarue, J. and C. Magnan, *Free fatty acids and insulin resistance*. *Curr Opin Clin Nutr Metab Care*, 2007. 10(2): p. 142-8.
56. Timmers, S., P. Schrauwen, and J. de Vogel, *Muscular diacylglycerol metabolism and insulin resistance*. *Physiol Behav*, 2008. 94(2): p. 242-51.
57. Roden, M., et al., *Mechanism of free fatty acid-induced insulin resistance in humans*. *J Clin Invest*, 1996. 97(12): p. 2859-65.

58. Amati, F., et al., *Skeletal muscle triglycerides, diacylglycerols, and ceramides in insulin resistance: another paradox in endurance-trained athletes?* *Diabetes*, 2011. 60(10): p. 2588-97.
59. Savage, D.B., K.F. Petersen, and G.I. Shulman, *Disordered lipid metabolism and the pathogenesis of insulin resistance.* *Physiol Rev*, 2007. 87(2): p. 507-20.
60. Randle, P.J., et al., *The glucose fatty-acid cycle. Its role in insulin sensitivity and the metabolic disturbances of diabetes mellitus.* *Lancet*, 1963. 1(7285): p. 785-9.
61. Krebs, M., et al., *Free fatty acids inhibit the glucose-stimulated increase of intramuscular glucose-6-phosphate concentration in humans.* *J Clin Endocrinol Metab*, 2001. 86(5): p. 2153-60.
62. Samuel, V.T., K.F. Petersen, and G.I. Shulman, *Lipid-induced insulin resistance: unravelling the mechanism.* *Lancet*, 2010. 375(9733): p. 2267-77.
63. Erion, D.M. and G.I. Shulman, *Diacylglycerol-mediated insulin resistance.* *Nat Med*, 2010. 16(4): p. 400-2.
64. Summers, S.A., *Sphingolipids and insulin resistance: the five Ws.* *Curr Opin Lipidol*, 2010. 21(2): p. 128-35.
65. Szendroedi, J., et al., *Effects of high-dose simvastatin therapy on glucose metabolism and ectopic lipid deposition in nonobese type 2 diabetic patients.* *Diabetes Care*, 2009. 32(2): p. 209-14.
66. Szendroedi, J., et al., *Muscle mitochondrial ATP synthesis and glucose transport/phosphorylation in type 2 diabetes.* *PLoS Med*, 2007. 4(5): p. e154.
67. Baecke, J.A., J. Burema, and J.E. Frijters, *A short questionnaire for the measurement of habitual physical activity in epidemiological studies.* *Am J Clin Nutr*, 1982. 36(5): p. 936-42.
68. DeFronzo, R.A., J.D. Tobin, and R. Andres, *Glucose clamp technique: a method for quantifying insulin secretion and resistance.* *Am J Physiol*, 1979. 237(3): p. E214-23.
69. Kraegen, E.W., et al., *In vivo insulin sensitivity in the rat determined by euglycemic clamp.* *Am J Physiol*, 1983. 245(1): p. E1-7.
70. Matsuda, M. and R.A. DeFronzo, *Insulin sensitivity indices obtained from oral glucose tolerance testing: comparison with the euglycemic insulin clamp.* *Diabetes Care*, 1999. 22(9): p. 1462-70.
71. Frayn, K.N., *Calculation of substrate oxidation rates in vivo from gaseous exchange.* *J Appl Physiol*, 1983. 55(2): p. 628-34.
72. Nowotny, B., et al., *Precision and accuracy of blood glucose measurements using three different instruments.* *Diabet Med*, 2012. 29(2): p. 260-5.
73. Phielix, E. and M. Mensink, *Type 2 diabetes mellitus and skeletal muscle metabolic function.* *Physiol Behav*, 2008. 94(2): p. 252-8.
74. Kumashiro, N., et al., *Cellular mechanism of insulin resistance in nonalcoholic fatty liver disease.* *Proc Natl Acad Sci U S A*, 2011. 108(39): p. 16381-5.
75. Neschen, S., et al., *Prevention of hepatic steatosis and hepatic insulin resistance in mitochondrial acyl-CoA:glycerol-sn-3-phosphate acyltransferase 1 knockout mice.* *Cell Metab*, 2005. 2(1): p. 55-65.
76. Mandarino, L.J., et al., *Differential regulation of intracellular glucose metabolism by glucose and insulin in human muscle.* *Am J Physiol*, 1993. 265(6 Pt 1): p. E898-905.

77. Hother-Nielsen, O., et al., *Effect of hyperglycemia per se on glucose turnover rates in patients with insulin-dependent diabetes*. *Metabolism*, 1993. 42(1): p. 86-93.
78. Vella, A., et al., *Glucose-induced suppression of endogenous glucose production: dynamic response to differing glucose profiles*. *Am J Physiol Endocrinol Metab*, 2003. 285(1): p. E25-30.
79. Vistisen, B., et al., *Effect of gender on lipid-induced insulin resistance in obese subjects*. *Eur J Endocrinol*, 2008. 158(1): p. 61-8.
80. Homko, C.J., P. Cheung, and G. Boden, *Effects of free fatty acids on glucose uptake and utilization in healthy women*. *Diabetes*, 2003. 52(2): p. 487-91.
81. Frias, J.P., et al., *Decreased susceptibility to fatty acid-induced peripheral tissue insulin resistance in women*. *Diabetes*, 2001. 50(6): p. 1344-50.
82. Nadal-Casellas, A., et al., *Sex-dependent differences in rat hepatic lipid accumulation and insulin sensitivity in response to diet-induced obesity*. *Biochem Cell Biol*, 2012. 90(2): p. 164-72.
83. Cnop, M., et al., *Relationship of adiponectin to body fat distribution, insulin sensitivity and plasma lipoproteins: evidence for independent roles of age and sex*. *Diabetologia*, 2003. 46(4): p. 459-69.
84. Galipeau, D.M., L. Yao, and J.H. McNeill, *Relationship among hyperinsulinemia, insulin resistance, and hypertension is dependent on sex*. *Am J Physiol Heart Circ Physiol*, 2002. 283(2): p. H562-7.
85. Hoeg, L.D., et al., *Lipid-induced insulin resistance affects women less than men and is not accompanied by inflammation or impaired proximal insulin signaling*. *Diabetes*, 2011. 60(1): p. 64-73.
86. Westerbacka, J., et al., *Women and men have similar amounts of liver and intra-abdominal fat, despite more subcutaneous fat in women: implications for sex differences in markers of cardiovascular risk*. *Diabetologia*, 2004. 47(8): p. 1360-9.
87. Randle, P.J., *Control of Insulin Secretion in Health and Disease*. *Isr Med J*, 1963. 22: p. 408-19.
88. Hegarty, B.D., et al., *The role of intramuscular lipid in insulin resistance*. *Acta Physiol Scand*, 2003. 178(4): p. 373-83.
89. Petersen, K.F. and G.I. Shulman, *Etiology of insulin resistance*. *Am J Med*, 2006. 119(5 Suppl 1): p. S10-6.
90. Summers, S.A., *Ceramides in insulin resistance and lipotoxicity*. *Prog Lipid Res*, 2006. 45(1): p. 42-72.
91. Adams, J.M., 2nd, et al., *Ceramide content is increased in skeletal muscle from obese insulin-resistant humans*. *Diabetes*, 2004. 53(1): p. 25-31.
92. Thrush, A.B., et al., *Skeletal muscle lipogenic protein expression is not different between lean and obese individuals: a potential factor in ceramide accumulation*. *J Clin Endocrinol Metab*, 2009. 94(12): p. 5053-61.
93. Consitt, L.A., J.A. Bell, and J.A. Houmard, *Intramuscular lipid metabolism, insulin action, and obesity*. *IUBMB Life*, 2009. 61(1): p. 47-55.
94. Straczkowski, M., et al., *Relationship between insulin sensitivity and sphingomyelin signaling pathway in human skeletal muscle*. *Diabetes*, 2004. 53(5): p. 1215-21.
95. Serlie, M.J., et al., *Short-term manipulation of plasma free fatty acids does not change skeletal muscle concentrations of ceramide and glucosylceramide in lean and overweight subjects*. *J Clin Endocrinol Metab*, 2007. 92(4): p. 1524-9.

96. Chavez, J.A., et al., *Acid ceramidase overexpression prevents the inhibitory effects of saturated fatty acids on insulin signaling*. *J Biol Chem*, 2005. 280(20): p. 20148-53.
97. Skovbro, M., et al., *Human skeletal muscle ceramide content is not a major factor in muscle insulin sensitivity*. *Diabetologia*, 2008. 51(7): p. 1253-60.
98. Schmitz-Peiffer, C., *Protein kinase C and lipid-induced insulin resistance in skeletal muscle*. *Ann N Y Acad Sci*, 2002. 967: p. 146-57.
99. Alkhateeb, H., et al., *Two phases of palmitate-induced insulin resistance in skeletal muscle: impaired GLUT4 translocation is followed by a reduced GLUT4 intrinsic activity*. *Am J Physiol Endocrinol Metab*, 2007. 293(3): p. E783-93.
100. Bergman, B.C., et al., *Localisation and composition of skeletal muscle diacylglycerol predicts insulin resistance in humans*. *Diabetologia*, 2012. 55(4): p. 1140-50.
101. Kruszynska, Y.T., et al., *Fatty acid-induced insulin resistance: decreased muscle PI3K activation but unchanged Akt phosphorylation*. *J Clin Endocrinol Metab*, 2002. 87(1): p. 226-34.
102. Storlien, L.H., et al., *Fish oil prevents insulin resistance induced by high-fat feeding in rats*. *Science*, 1987. 237(4817): p. 885-8.
103. Schmitz-Peiffer, C., D.L. Craig, and T.J. Biden, *Ceramide generation is sufficient to account for the inhibition of the insulin-stimulated PKB pathway in C2C12 skeletal muscle cells pretreated with palmitate*. *J Biol Chem*, 1999. 274(34): p. 24202-10.
104. Gorden, D.L., et al., *Increased diacylglycerols characterize hepatic lipid changes in progression of human nonalcoholic fatty liver disease; comparison to a murine model*. *PLoS One*, 2011. 6(8): p. e22775.
105. Itani, S.I., et al., *Lipid-induced insulin resistance in human muscle is associated with changes in diacylglycerol, protein kinase C, and IkappaB-alpha*. *Diabetes*, 2002. 51(7): p. 2005-11.
106. Chalfant, C.E., et al., *Protein kinase Ctheta expression is increased upon differentiation of human skeletal muscle cells: dysregulation in type 2 diabetic patients and a possible role for protein kinase Ctheta in insulin-stimulated glycogen synthase activity*. *Endocrinology*, 2000. 141(8): p. 2773-8.
107. Itani, S.I., et al., *Involvement of protein kinase C in human skeletal muscle insulin resistance and obesity*. *Diabetes*, 2000. 49(8): p. 1353-8.
108. Kim, Y.B., et al., *Insulin-stimulated protein kinase C lambda/zeta activity is reduced in skeletal muscle of humans with obesity and type 2 diabetes: reversal with weight reduction*. *Diabetes*, 2003. 52(8): p. 1935-42.
109. Gray, S., et al., *Increased skeletal muscle expression of PKC-theta but not PKC-alpha mRNA in type 2 diabetes: inverse relationship with in-vivo insulin sensitivity*. *Eur J Clin Invest*, 2003. 33(11): p. 983-7.
110. Neri, L.M., et al., *Protein kinase C isoforms and lipid second messengers: a critical nuclear partnership?* *Histol Histopathol*, 2002. 17(4): p. 1311-6.

Danksagung

Meinem Doktorvater, Herrn Professor Dr. med. Michael Roden, danke ich für das Überlassen des Themas und, dass ich am Institut für Klinische Diabetologie, Deutsches Diabetes-Zentrum die vorliegende Dissertation anfertigen durfte. Er gab mir die Möglichkeit, Einblicke in wissenschaftliche Untersuchungen zu gewinnen und auf einem für mich als Zahnärztin fachfremden Gebiet zu arbeiten. Professor Roden begleitete das Erstellen der Arbeit mit viel Geduld sowie konstruktiver Kritik. Ohne seine wohlwollende Unterstützung wäre diese Arbeit nicht möglich geworden.

Mein besonderer Dank gilt Frau Dr. med. Julia Szendroedi, die mir beim Bewältigen der Thematik immer freundschaftlich und hilfsbereit zur Seite stand; sie hatte stets ein offenes Ohr für mich. Ich habe bei ihr sehr viel lernen dürfen.

Weiterhin bedanke ich mich bei allen Mitarbeitern des Deutschen Diabetes-Zentrums, die mir mit ihrem Fachwissen zur Verfügung standen.

Von ganzen Herzen danke ich meinen Eltern und meiner Schwester, die während meines Promotionsvorhabens nie aufgehört haben mich zu unterstützen und zu ermutigen. Sie sind maßgeblich am Gelingen dieser Arbeit beteiligt. Meinen Eltern widme ich diese Arbeit.

Zuletzt danke ich meinem Freund Mark, der während des Erstellens der Arbeit auf mich sehr oft verzichten musste. Er hat mich sehr verständnisvoll unterstützt und stand mir immer liebevoll zur Seite.

Eidesstattliche Versicherung

Ich versichere an Eides statt, dass die Dissertation selbständig und ohne unzulässige fremde Hilfe erstellt worden ist und die hier vorgelegte Dissertation nicht von einer anderen Medizinischen Fakultät abgelehnt worden ist.

Düsseldorf, 24.05.2014

Janette Müller (geb. Decker)